

Characterisation of a cascaded power supply for use with multi-GEM stacks

P. Gasik^{1,2}, L. Fabbietti^{1,2} and the ALICE Collaboration

¹Physik Department E62, TU München, 85748 Garching, Germany;

²Excellence Cluster ‘Origin and Structure of the Universe’, 85748 Garching, Germany

The ALICE Collaboration will undertake a major upgrade of the detector apparatus in view of the LHC Runs 3 and 4 (2021 to 2029). In particular, new readout chambers will be installed in the TPC, replacing currently used Multi Wire Proportional Chambers with Gas-Electron-Multiplier-(GEM)-based detectors. New chambers employ stacks of four GEM foils, which require a High-Voltage system with eight HV power channels. This can be realised by employing a passive voltage divider (resistor chain), eight independent HV channels (each referring its potential to ground) or a novel system of eight “cascaded” HV channels that sit on top of each other (each referring its potential to the channel below) generating a cascade of high voltages.

In the first scenario, all fields and GEM voltages are defined by the resistor values and cannot be changed easily during the detector operation. Independent HV channels give full flexibility in choosing GEM voltages, however, the potential differences between subsequent channels may increase substantially in case of a spark discharge event or emergency shutdown of all channels caused by a power supply trip. Measurements performed at the Technical University of Munich have shown that the time difference between switching subsequent HV channels off may reach several hundreds of milliseconds. This can easily result in large potential differences across GEMs causing their irreversible damage.

The cascaded PS system was characterised in terms of its reaction on a discharge event and different tripping modes. Measurements were performed with a prototype delivered by ISEG GmbH. All tests were done using a GEM-PCB Simulator [1], an equivalent of a ~ 0.17 m² large quadruple GEM stack of an ALICE Inner Readout Chamber. Measurements included realistic cable lengths and protection resistor values. Differential voltages on the HV channels were monitored with 1:10 and 1:100 scope test probes via decoupling capacitors. Self-made 1:1000 probes were used to monitor absolute voltages on a long-timescale.

A discharge event is induced using a Gas Discharge Tube connected across a capacitor representing a single GEM segment (~ 5 nF). We do not measure any significant over-voltages across GEM foils and GEM segments other than the sparking one. Small voltage variations observed in the subsequent GEMs are due to the capacitive coupling of the foils and may cause increase of the potential difference across a GEM at a single-volts level.

The time-characteristics of the cascaded power supply is measured for different tripping modes after detection of an overcurrent:

- turn channel off with ramp,
- turn channel off without ramp,
- turn all channels off without ramp.

A relay is used to create a short across a single GEM segment and trigger a trip.

In case of the single-channel reaction, we do not observe any significant voltage increase across non-tripping GEMs. Occasional few-volts increase due to the capacitive coupling of the subsequent foils does not pose a threat to the GEMs. It is worth to mention that in case no software delay is specified between an overcurrent detection and turning the HV channel off, the intrinsic system delay varies between 10 and 20 ms. This means that the voltage across GEM may be reduced immediately after spark detection, before the nominal potential difference is reached (the typical re-charging time of a 100 cm² segment, powered via 10 M Ω protection resistor, is ~ 200 ms).

The most crucial issue is a measurement of the last tripping mode, when all channels are switched off without ramp (emergency shutdown of the PS). By construction, no overvoltage is expected across any of GEMs, as the HV channels of the cascaded PS are stacked in a row as in case of the passive voltage divider. The latter is confirmed in our tests where we measure time delays between switching off subsequent channels. In a series of measurements where the emergency shut down is triggered in different HV channels, we observe that all channels are switched off at the same moment (see Fig. 1) and no overvoltage is created across any of the GEMs in the stack.

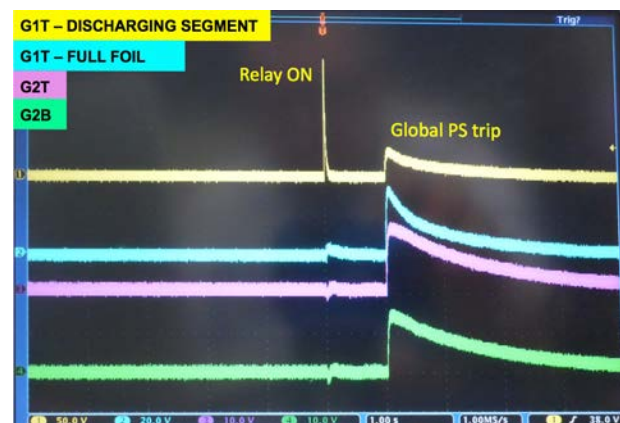


Figure 1: Reaction of the cascaded PS to an overcurrent detected in one of the channels (Relay ON). All channels are switched off at the same moment (within <1 ms). A one-second reaction-delay was set in the PS software.

In summary, the measurements presented in this report assure safe operation of GEM-stacks with the cascaded power supplies that are considered as a baseline PS system for the ALICE TPC upgrade.

References

- [1] P. Gasik, “Quadruple GEM-PCB Simulator”, GSI Scientific Report 2016, doi:10.15120/GR-2017-1.

Experiment beamline: none

Experiment collaboration: CERN-ALICE

Experiment proposal: none

Accelerator infrastructure: CERN-LHC

PSP codes: none

Grants: Excellenzcluster Universe ‘Origin and Structure of the Universe’ DFG EClust 153, BMBF ALICE ‘Verbundprojekt 05P2015’

Strategic university co-operation with: none

Measurement of J/ψ production as a function of event multiplicity in pp collisions at $\sqrt{s} = 13$ TeV with ALICE*

S. Weber^{1,2}, for the ALICE collaboration

¹GSI, Darmstadt, Germany; ²TU Darmstadt, Germany

The event multiplicity dependent production of charmonium gives insight into QCD processes and particularly the interplay between the hard and soft mechanisms in particle production. ALICE has performed multiplicity dependent measurements of inclusive J/ψ production at mid and forward rapidity in pp collisions at $\sqrt{s} = 7$ TeV [1], reaching multiplicities of about 4 times the mean value. The results are consistent with a stronger than linear increase with multiplicity, similar to results for open-charm hadrons and J/ψ originating from beauty-hadron decays (“non-prompt” J/ψ) [2].

A new measurement of J/ψ production as a function of event multiplicity was performed with the ALICE detector [3] in pp collisions at $\sqrt{s} = 13$ TeV. Using a trigger on high event multiplicities, based on a large deposited charge in the ALICE V0 scintillator arrays at forward and backward rapidity, mid-rapidity multiplicities of about 7 times the mean value in minimum bias collisions were reached. High p_T J/ψ ($p_T > 8$ GeV/c) were obtained from data triggered by the EMCAL electromagnetic calorimeter. The signal was extracted from the dielectron decay channel in the ALICE central barrel. Particle identification was performed with the TPC detector, for high p_T , together with the EMCAL PID information.

Figure 1 shows the self-normalized J/ψ yield as a function of charged-particle multiplicity in four p_T bins. A stronger increase for higher p_T is observed, in qualitative agreement with predictions from the PYTHIA8 model [4]. Within this model, the increase of J/ψ production can be understood from production in multi-parton interactions (MPI).

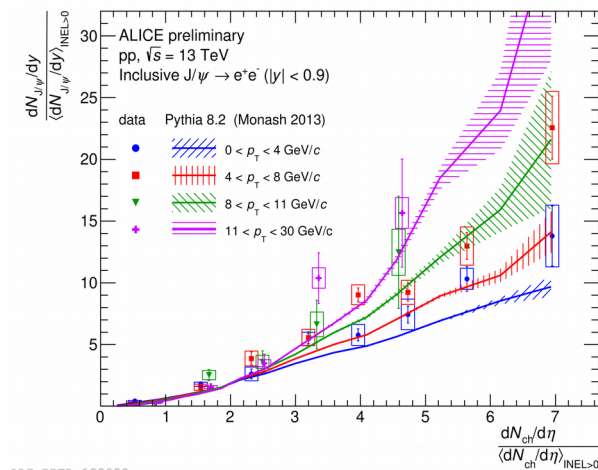


Figure 1: Multiplicity dependence of inclusive J/ψ production at mid-rapidity at $\sqrt{s} = 13$ TeV in four transverse momentum bins, comparison to PYTHIA8.

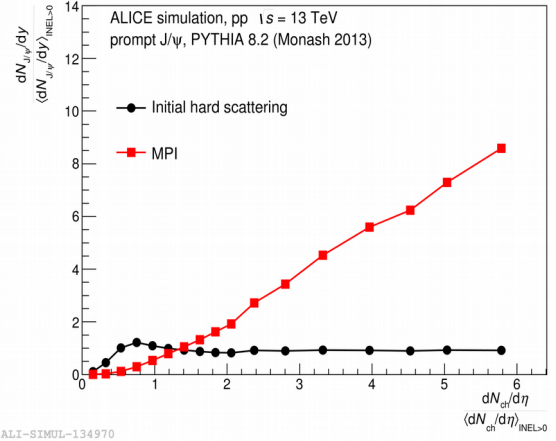


Figure 2: PYTHIA8 prediction for multiplicity dependence of prompt J/ψ production from initial hard scatterings and from MPI in pp collisions at $\sqrt{s} = 13$ TeV.

Figure 2 shows the PYTHIA8 prediction for the self-normalized yield of prompt J/ψ (excluding beauty-hadron decays) as a function of charged-particle multiplicity for J/ψ produced in the initial hard scattering of the event, and for J/ψ produced in subsequent ones from the MPI framework. It can be seen that initially produced J/ψ are independent of the charged-particle multiplicity, so the contribution of J/ψ from MPI is vital for the understanding of the data.

References

- [1] B. Abelev, et al., Phys. Lett. B712 (2012) 165–175.
- [2] J. Adam, et al., JHEP 09 (2015) 148.
- [3] K. Aamodt, et al., JINST 3 (2008) S08002.
- [4] T. Sjostrand, S. Mrenna, P. Z. Skands, Comput. Phys. Commun. 178 (2008) 852–867.

*Work supported by BMBF, GSI, HGS-HIRE, HIC4-FAIR, H-QM, TU Darmstadt

Σ^0 baryon production in pp collisions at $\sqrt{s} = 13$ TeV measured with the ALICE experiment*

A. Mathis^{1,2} and L. Fabbietti^{1,2}, for the ALICE collaboration

¹Technische Universität München, Physik Department E62, Garching, Germany

²Excellence Cluster ‘Origin and Structure of the Universe’, Garching, Germany

To present day, only very little is known about the interaction between Σ baryons and nucleons (Σ -N). This is due to the fact that up to now, Σ hypernuclei have not been observed yet and moreover, scattering data for Σ hyperon beams are scarce. Hence, the Σ -N interaction remains to be probed. For other hyperons, the situation is somewhat better, in particular for the case of the Λ . Recently, much progress has been made for the case of the Λ -N interaction by employing femtoscopy as a complementary method compared to scattering data. In the context of femtosopic measurements, it is also interesting to quantify the feed-down from the Σ^0 which decays almost exclusively into a Λ baryon and a photon [1] to the final state of interest containing a Λ . At low collision energies close to the NN threshold, the production cross-sections $\sigma_\Lambda/\sigma_\Sigma \approx 10$ [2] suggest a feed-down of $\sim 10\%$. For larger energies, however, according to isospin considerations, the ratio is expected to approach 1/3 [3] as the Λ is represented in an isospin singlet state while the Σ^0 belongs to an isospin triplet representation. Hence, if sufficient energy is available in the reaction, three different Σ states can be excited but only one Λ state.

A study of the Σ -N, and the hyperon-nucleon interaction in general is also of interest in the context of the study of the content of neutron stars. Even though, as recently demonstrated, gravitational wave observations of binary neutron star mergers are a powerful tool to determine the neutron star equation of state (EOS), the latter still remains a puzzle. In particular, for the description of such a system in the presence of hyperons a thorough understanding of the hyperon-nucleon interaction is mandatory.

As a first step, we measure the production of the Σ^0 baryon at an unprecedented high energy of $\sqrt{s} = 13$ TeV in pp collisions with the ALICE detector. For the analysis, all available data are employed, which account to about 1×10^9 events collected with a minimum-bias trigger. For the reconstruction of the Σ^0 the dominant decay channel $\Sigma^0 \rightarrow \Lambda \gamma$ is exploited. The Λ is then subsequently identified via its decay into a charged pion and a proton (BR $\sim 63.9\%$ [1]) employing the dE/dx information provided by the ALICE Time Projection Chamber. The energy of the photon is typically too low to allow for the employment of ALICE’s electromagnetic calorimeter. Instead, the photon conversion method is used which relies on the identification of the dielectron pair produced in the conversion of a photon in the detector material, $\gamma \rightarrow e^+e^-$. For the case of ALICE, the corresponding probability is about 8%. The four-momentum vector of the Λ is then combined with a dielectron pair and the resulting invari-

ant mass is depicted in Fig. 1. The background is described by a forth-order polynomial (dotted line) and the signal is parametrized by a single Gaussian.

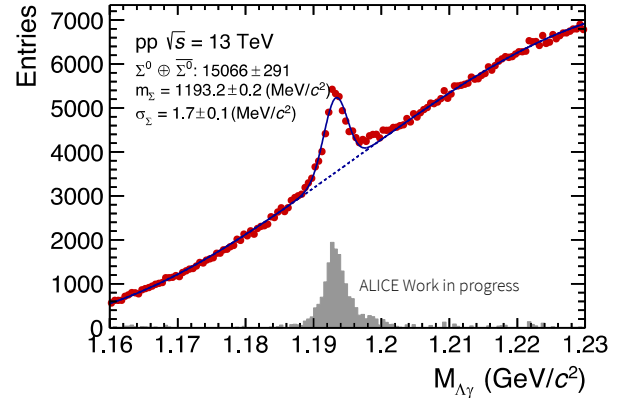


Figure 1: Invariant mass of the Λ and a dielectron pair. The dotted line depicts the combinatorial background and the signal is parametrized by a Gaussian. The grey histogram displays the signal after subtraction of the background.

A global fit of the spectrum yields in total about 15,000 Σ^0 baryons candidates at a signal-to-noise ratio of about 0.2. After correcting the spectra for acceptance and efficiency, this analysis will yield the Σ^0 production cross-section and the Σ^0/Λ ratio at an unprecedented high energy of $\sqrt{s} = 13$ TeV together with a comparison to event generators such as PYTHIA [4]. Moreover, with more data being reconstructed, the feasibility of p- Σ^0 femtoscopy will be checked, possibly allowing to constrain the Σ -N interaction for the first time. Additionally, with the available statistics, a study of all relevant decay channels ($\Sigma^0 \rightarrow \Lambda \gamma$, $\Sigma^0 \rightarrow \Lambda \gamma \gamma$ and $\Sigma^0 \rightarrow \Lambda e^+e^-$ [1]) may be at hand and the feasibility will be explored, which for the first time would allow for a relative measurement of the corresponding branching ratios.

References

- [1] K.A. Olive *et al.*, Chin. Phys. C, 38, 0900001 (2014).
- [2] P.Kowina *et al.*, Eur. Phys. J. A 22, 293-299 (2004).
- [3] H.Landolt, R.Börnstein, Landolt-B.12, (1988).
- [4] T. Sjöstrand, S. Mrenna, and P. Skands, Journal of High Energy Physics 2006 no. 05, (2006) 026.

*) Work supported by the DFG Exzellenzcluster Universe, ‘‘Origin and Structure of the Universe’’ (DFG EClust 153), BMBF ALICE ‘‘Verbundprojekt 05P2015’’ and the Collaborative Research Center ‘‘Neutrinos und Dunkle Materie in der Astro- und Teilchenphysik (NDM)’’ (SFB 1258).

Baryon Femtoscopy in p–Pb Collisions at 5.02 TeV

B. Hohlweger^{1,2} and L. Fabbietti^{1,2}, for the ALICE collaboration

¹Technische Universität München, Physik Department E62, Garching Germany, ²Excellence Cluster 'Origin and Structure of the Universe', Garching, Germany

Understanding the interaction of hyperons at finite densities is fundamental in order to understand the role of strange degrees of freedom in the Equation of State (EoS) of neutron stars. Scattering data for hyperons does not allow to discriminate between models of baryon-hyperon interaction. Therefore, femtoscopy has been proposed to study the interaction of these pairs. The observable in femtoscopic analysis is the two-particle correlation function, defined as

$$C(\mathbf{p}_1, \mathbf{p}_2) = \frac{P(\mathbf{p}_1, \mathbf{p}_2)}{P(\mathbf{p}_1)P(\mathbf{p}_2)} = C(k) = \int S(\mathbf{r}, k) |\psi(\mathbf{r}, k)|^2 d\mathbf{r}, \quad (1)$$

where $P(\mathbf{p}_1, \mathbf{p}_2)$ is the conditional probability of finding a particle pair with a momentum \mathbf{p}_1 and \mathbf{p}_2 in the same event, while $P(\mathbf{p}_i)$ is the single particle probability of independently finding the particles with momentum \mathbf{p}_i . This quantity can also be viewed as a function of the relative momentum k in the pair center of mass frame and is related to the product of source function $S(\mathbf{r}, k)$ and wave function $\psi(\mathbf{r}, k)$ [2]. The sensitivity to the interaction arises from the wave function, which is obtained by solving the Schrödinger equation incorporating the interaction potential of a given pair. The source is typically described by a Gaussian distribution and is assumed to be the same for all baryon pairs.

In a recent study in p–Nb collisions at $\sqrt{s} = 3.5$ GeV [1] and in pp collisions at $\sqrt{s} = 7$ TeV it has been shown that the correlation function for p– Λ pairs develops a sensitivity to different scattering parameters. It was however apparent that more statistics would allow for stronger constraints on different models and for this purpose, the analysis was extended to data from p–Pb collisions at $\sqrt{s_{NN}} = 5.02$ TeV. After applying event selection criteria, around 600 million events are available to analyse pairs of p– Λ and p– Ξ . The Λ hyperon is identified via its decay into a charged pion and proton (BR $\sim 63.9\%$), which subsequently are identified by the dE/dx measurement in the Time Projection Chamber (TPC). The resulting sample has a purity of around 96%. The Ξ hyperon is identified via its decay into a Λ and a pion (BR $\sim 99.9\%$). A first signal of Ξ 's in the invariant mass distribution is depicted in Fig. 1, where a purity of around 87% is reached. The experimental correlation function for p–p, p– Λ and p– Ξ pairs is then obtained by constructing the relative momentum distribution from pairs in the same event $N_{SE}(k)$ and of uncorrelated pairs $N_{ME}(k)$ where each particle is from a different event. The correlation function is obtained by dividing the $N_{SE}(k)$ by $N_{ME}(k)$.

The Correlation Analysis Tool using the Schrödinger Equation (CATS) [3] framework has been employed in the calculation of the proton-hyperon interaction. For p– Λ pairs the interaction has been described by χ_{EFT} potentials at LO and NLO. In the case of p– Ξ pairs a preliminary

local potential from the HAL Lattice QCD collaboration [4] has been adopted. The correlation function, as shown in Eq. (1), depends both on the source size and the underlying potential. Studying the source with p–p pairs, where the interaction potential is well known, allows to reduce the uncertainty arising from the size of the emitting source and permits to set tighter constraints on the strong potential of more exotic pairs as baryon-hyperon or hyperon-hyperon. In the p–Pb system the size of the source depends on the impact parameter and its variations are expected to be larger than in the elementary collisions. The geometry of the emitting source can be studied by using the p–p correlation function binned in several multiplicity classes. The results of this study will provide the necessary input to perform a final combined fit of baryon-baryon pairs in the p–Pb collision system and to ultimately constrain the interaction potentials for baryon-hyperon pairs.

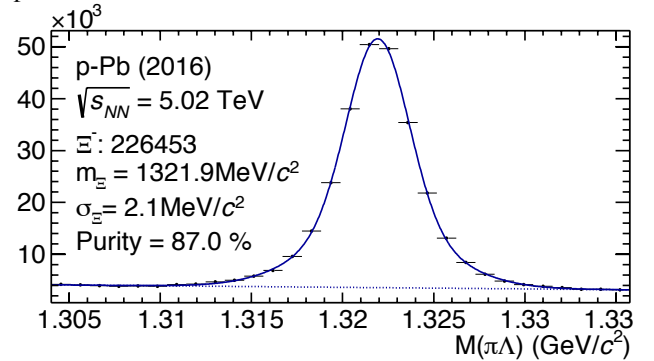


Figure 1: Ξ – Signal reconstructed in the $\Lambda \pi$ channel from p–Pb Data at $\sqrt{s_{NN}} = 5.02$ TeV.

References

- [1] HADES Collaboration, Λp interaction studied via Femtoscopy in p+Pb recations at $\sqrt{s_{NN}} = 3.18$ GeV, Phys. Rev. C, 94, 025201 (2016)
- [2] Michael Annan Lisa and Scott Pratt et al, Femtoscopy in Relativistic Heavy Ion Collisions: Two Decades of Progress, Annual Review of Nuclear and Particle Science, 55, 357-402 (2005)
- [3] D.L. Mihaylov, V. Mantovani Sarti et. al, A femtoscopic Correlation Analysis Tool using the Schrödinger equation (CATS), arXiv:1802.08481
- [4] Kenji Sasaki, Sinya Aoki et. al, Baryon interactions from lattice QCD with physical masses -- S=-2 sector, arXiv:1702.06241

Experiment collaboration: CERN-ALICE

Accelerator infrastructure: CERN-LHC

Grants: SFB: Sonderforschungsbereich 1258 "Neutrinos und Dunkle Materie in der Astro- und Teilchenphysik (NDM)"

Strategic university co-operation with: TU München

Low-mass dielectron production in pp collisions at $\sqrt{s} = 13$ TeV with ALICE*

I. Vorobyev^{1,2}, A. Dashi^{1,2}, O. Vazquez Doce^{1,2}, T. Dahms^{1,2}, for the ALICE collaboration

¹Excellence Cluster Universe, Technische Universität München, Garching, Germany;

²Physik Department, Technische Universität München, Garching, Germany

Electron–positron pairs (dielectrons) are a unique experimental tool to investigate the hot and dense medium created in ultra-relativistic heavy-ion collisions. Such pairs are produced during all stages of the collision and do not interact strongly. Therefore, they carry information about the medium properties and the whole space-time evolution of the system.

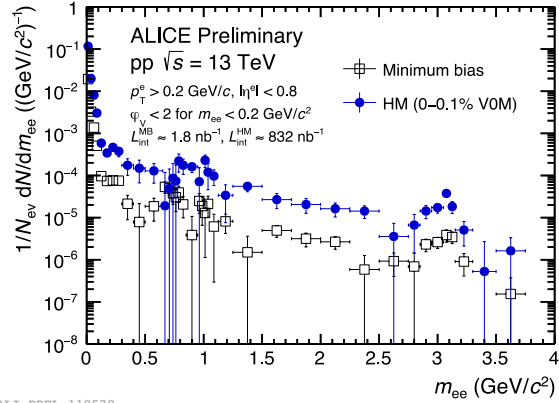
Measurements of dielectron production in minimum-bias proton–proton (pp) collisions provide an important vacuum reference for any modifications observed in heavy-ion collisions. Moreover, the measurement of e^+e^- pairs from semileptonic decays of correlated heavy-flavour hadrons in the intermediate-mass region ($1.1 < m_{ee} < 2.9$ GeV/ c^2) allow further studies and understandings of the primordial heavy-flavour production. Recent studies of pp collisions with high charged-particle multiplicities showed interesting results similar to the observations previously made in heavy-ion collisions. Measurements of low-mass dielectrons could provide further insight into the underlying physics processes.

The dielectron analysis is performed in the central barrel spectrometer of ALICE [1]. For both multiplicity classes the collision events are triggered on by the V0 detector. Charged particle tracks are reconstructed with the Inner Tracking System (ITS) and the Time Projection Chamber (TPC) in the kinematic range $|\eta_e| < 0.8$ and $p_{T,e} > 0.2$ GeV/ c . Specific energy loss in the TPC and the time-of-flight information from the TOF detector are used for the electron identification.

All electron and positron candidates are paired considering the combinations with opposite but also same charge. The combinatorial background is estimated via the geometric mean of same-sign pairs within the same event. Conversions of real photons in the detector material are removed from the raw signal by their orientation relative to the magnetic field. The resulting raw dielectron spectra in high-multiplicity and minimum-bias events are shown in Fig. 1.

References

- [1] ALICE Collaboration, JINST3 (2008) 08002
- [2] ALICE Collaboration, Phys. Lett. B 753, 319 (2016)
- [3] ALICE Collaboration, JHEP 09, 148 (2015)



ALI-PREL-119579

Figure 1: Raw dielectron spectra in minimum-bias (black) and high-multiplicity (blue) events.

The current work focuses on the analysis of approximately 5 times more pp collision data from 2016. The raw dielectron spectra will be corrected for the reconstruction efficiencies using detailed Monte Carlo simulations. The results will be compared to the expectations from all known hadronic sources, i.e. the hadronic cocktail, contributing to the dielectron spectrum in the ALICE central barrel acceptance. For the high-multiplicity cocktail, the light-flavour hadron p_T distributions are adjusted according to the measured modification of charged hadron p_T spectra [2]. The contribution of correlated semileptonic decays of open charm and bottom mesons is estimated with PYTHIA and POWHEG simulations. For the multiplicity dependence, the results on D-meson production as a function of p_T and multiplicity [3] are used to weight the open charm and bottom contributions. In the intermediate mass range the data will be fitted with PYTHIA and POWHEG templates of open charm and bottom production, which will allow us to extract the heavy-flavour cross sections. Finally, assuming the equivalence between the fraction of real direct photons and the fraction of virtual direct photons at zero mass, the former can be extracted from the dielectron spectrum measured at small invariant mass.

* Work supported by Excellence Cluster “Origin and Structure of the Universe”, DFG EClust 153 and BMBF ALICE: “Verbundprojekt 05P2015”

Production of electrons from semileptonic heavy-flavour hadron decays in proton-proton and heavy-ion collisions measured with ALICE at the LHC*

*C. de Conti¹, A. Dubla^{2,3}, M. Faggin⁵, S. Hornung^{2,3}, S. P. Rode⁴,
for the ALICE collaboration*

¹Universidade de Sao Paulo, Brasil; ²GSI, Darmstadt, Germany; ³Heidelberg university, Germany; ⁴Indian Institute of Technology Indore, India; ⁵University of Padova

The transverse momentum (p_T) spectra and the nuclear modification factor (R_{AA}) of electrons from semileptonic heavy-flavour hadron decays is measured in Pb-Pb collisions at $\sqrt{s_{NN}} = 5.02$ TeV and in Xe-Xe collisions at 5.44 TeV. The modification of the p_T spectra is studied at mid-rapidity ($|y| < 0.8$) in the p_T interval 0.5-6 GeV/c. The R_{AA} is calculated using the proton-proton (pp) reference cross-section measured in the same p_T interval and at the same center-of-mass energy as for the Pb-Pb measurement. For the Xe-Xe R_{AA} the pp reference was obtained using an interpolation procedure. In addition, the production cross-section was also measured in pp collisions at $\sqrt{s} = 7$ TeV and $\sqrt{s} = 13$ TeV.

Introduction

In ultra-relativistic heavy-ion collisions at the Large Hadron Collider (LHC) a strongly-interacting matter, characterised by high energy density and temperature, is produced. Under these conditions, the formation of a deconfined state of quarks and gluons, the Quark-Gluon Plasma (QGP), is predicted by Quantum ChromoDynamic (QCD) calculations on the lattice. The production of heavy quarks, i.e. charm (c) and beauty (b) is characterised by a timescale shorter than $1/(2*m_c, b)$, where m is the mass of the quark. This timescale (e.g. ~ 0.08 fm/c for charm) is expected to be smaller than the QGP thermalization time ($\sim 0.6-1$ fm/c). Heavy quarks interact with the QGP and suffer energy loss while propagating through it. The modification of the p_T spectra in heavy-ion collisions with respect to those in pp collisions at the same centre-of-mass energy is quantified by the nuclear modification factor R_{AA} , defined as:

$$R_{AA} = \frac{(dN_{AA}/dp_T)}{(d\sigma_{pp}/dp_T) \cdot \langle T_{AA} \rangle} \quad (1)$$

where dN_{AA}/dp_T is the measured yield in heavy-ion collisions and $d\sigma_{pp}/dp_T$ is the corresponding cross-section in pp collisions.

* Work supported by GSI, BMBF, DST-DAAD and HGS-HIRE and ISOQUANT.

The average nuclear overlap function, $\langle T_{AA} \rangle$, is estimated via Glauber model calculations and is proportional to the

average number of binary nucleon-nucleon collisions in nucleus-nucleus (AA) collisions in a given centrality class.

Low- p_T heavy-flavour measurements are very important to test the binary scaling of the heavy-quark production in heavy-ion collisions. In addition, they allow to extract information about possible influences from the initial state effects, like the modification of the parton distribution functions at the LHC energies. They also carry information about different hadronisation mechanisms, namely the fragmentation in the vacuum and the coalescence in the medium. At high- p_T heavy quarks are sensitive to the medium energy density, through the mechanism of parton energy loss.

Results

The p_T -differential cross section for electrons from heavy-flavour hadron decays at mid-rapidity in pp collisions at $\sqrt{s} = 5.02, 7$ and 13 TeV using the photonic-electron tagging are shown in the left, middle and right panel of Figure 1, respectively. The statistical uncertainties are shown as vertical bars and the systematic uncertainties as empty boxes. The dashed line indicate the central value of the FONLL calculation [1]. The full systematic band of the model originates from the variation of the factorization and normalization scale as well as the heavy-quark masses and the uncertainty of the parton distribution function (PDF) used. In the lower panels of Figure 1 the ratios of the experimental measurements with the central value of the FONLL calculations are shown. Within the systematic uncertainties of the measurement and the calculation, the theoretical calculation is in good agreement with the data. The measured cross sections are close to the upper edge of the FONLL uncertainty band. Figure 2 shows the R_{AA} of electrons from heavy-flavour hadron decays at mid-rapidity ($|y| < 0.8$) as a function of p_T in Pb-Pb collisions at $\sqrt{s_{NN}} = 5.02$ TeV for the 0-10% centrality class. The new low p_T measurement is shown together with the high p_T results obtained using the TPC+EMCal detectors to identify the electron (orange closed marker) [2].

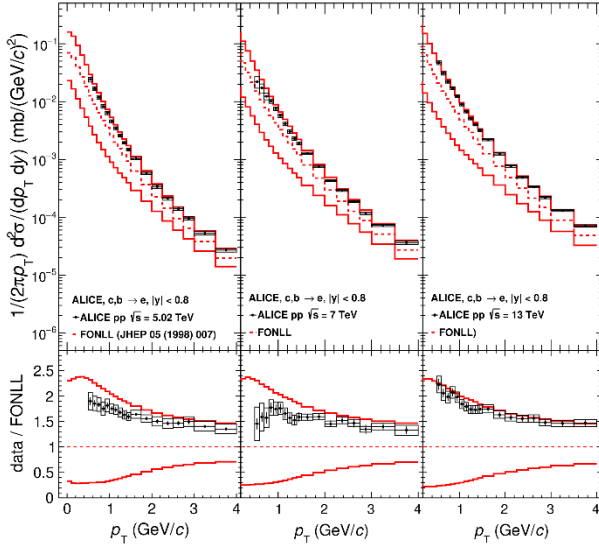


Figure 1: p_T -differential cross section of electrons from heavy-flavour hadron decays at mid-rapidity in pp collisions at $\sqrt{s} = 5.02$ TeV, 7 TeV and 13 TeV compared to pQCD calculations.

The statistical and systematic uncertainties of the spectra in Pb-Pb and pp were propagated as independent uncertainties. The uncertainty on the normalisation (3%) is the uncertainty on $\langle T_{AA} \rangle$ and it is represented by a filled box at $R_{AA} = 1$. At high p_T , the R_{AA} is below unity, showing a suppression of the yield of electrons from heavy-flavour hadron decays with respect to pp due to the energy loss of heavy quarks in the QCD medium.

For $p_T < 1.5$ GeV/c, the data is compatible with unity

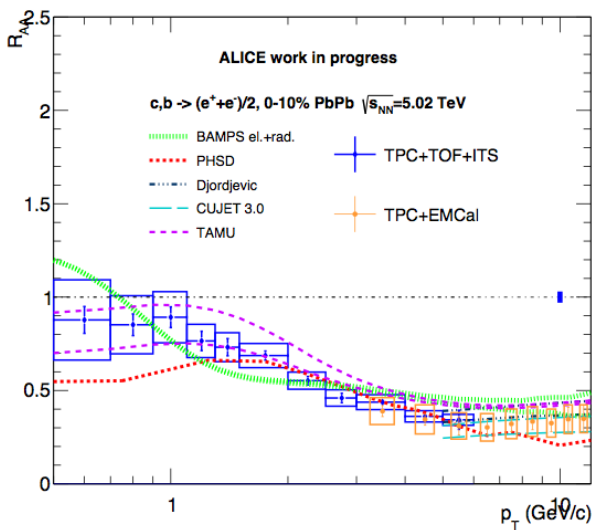


Figure 2: Heavy-flavour hadron decay electron R_{AA} at mid-rapidity as a function of p_T in central Pb-Pb collisions at $\sqrt{s_{NN}} = 5.02$ TeV compared to models [3-6].

within systematic uncertainties. Models which include

shadowing, like TAMU [4], predict an R_{AA} smaller than one even at low p_T and are in good agreement with the experimental measurement.

In Figure 3 the R_{AA} of electrons from heavy-flavour hadron decays at mid-rapidity ($|y| < 0.8$) as a function of p_T in Xe-Xe collisions at $\sqrt{s_{NN}} = 5.44$ TeV is shown in the 0-20% centrality interval. The measurement is important to further study and constrain the energy loss dependence of the heavy quarks with respect to the size of the colliding nuclei. In addition, the modification of the parton distribution functions using a similar centre-of-mass collision energy but different nuclei can be investigated. Also in this case the uncertainty on the normalisation (9%) is the uncertainty on $\langle T_{AA} \rangle$ and it is represented by a filled box at $R_{AA} = 1$. When compared with the R_{AA} in Pb-Pb collisions an indication of a smaller suppression in Xe-Xe collision is observed.

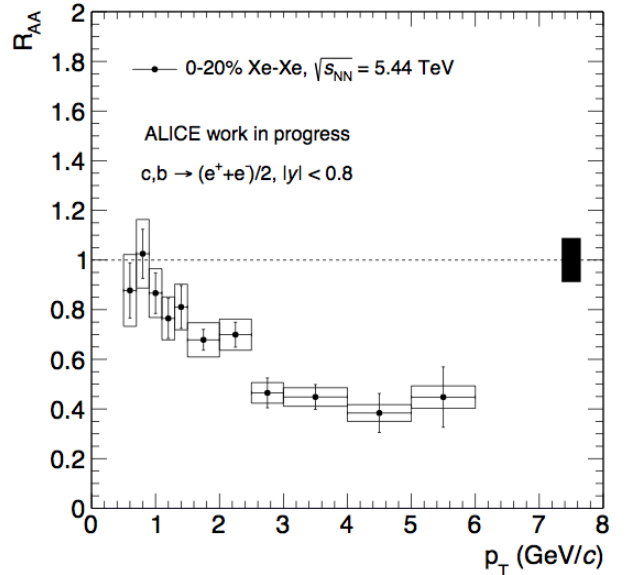


Figure 3: Heavy-flavour hadron decay electron R_{AA} at mid-rapidity as a function of p_T in the 0-20% centrality class in Xe-Xe collisions at $\sqrt{s_{NN}} = 5.44$ TeV.

References

- [1] M. Cacciari et al., JHEP 05 (1998) 007
- [2] ALICE Collaboration, Nucl. Phys. A 967 (2017)
- [3] J. Uphoff et al., J.Phys.Conf.Ser. 509 (2014) 012077
- [4] M. He et al., Phys.Lett. B735 (2014) 445–450
- [5] W. Cassing et al., Phys.Rev. C78 (2008) 034919
- [6] J. Xu, J. Liao et al. Chin. Phys. Lett. 32 no. 9, (2015)

Quality assurance of GEM-based readout chambers for the Time Projection Chamber of ALICE

L. Kreis^{1,2}, M. Habib^{1,3}, A. Harlenderová^{1,2}, S. Hornung^{1,2}, J. Hehner¹, S. Masciocchi^{1,2}, D. Miśkowiec¹, T. Rudzki^{1,2}, B. Voss¹, the ALICE Collaboration

¹GSI, Darmstadt, Germany; ²Ruprecht-Karls-Universität Heidelberg, Germany; ³Technische Universität Darmstadt, Germany

In the upcoming long shutdown period of the LHC, ALICE will be upgraded to be able to record Pb–Pb collisions at an event rate of 50 kHz. The current readout chambers of the Time Projection Chamber (TPC) are multiwire proportional chambers, which limit the event rate to 3 kHz. A new readout based on gas electron multipliers (GEM) is currently under construction. A stack of four GEMs is used, where two large pitch foils are sandwiched between two standard pitch foils.

These new readout chambers will allow continuous data-taking during LHC Run 3 and 4. The ALICE TPC readout chambers come in two sizes: the inner readout chambers and the outer readout chambers (OROC) with one stack and three GEM stacks, respectively. The TPC upgrade project is distributed between different institutes. GSI is responsible for the framing of GEMs from the largest stack and for the OROC assembly.

After the assembly, several parameters are measured to guarantee a stable operation of the chambers at the LHC, while maintaining the performance of the current setup [1]. The ion backflow (defined as the ratio of the cathode current and the current on the pad plane $IBF = I_{cathode} / I_{pads}$ at an effective gas gain of 2000 has to be below 1%. The local energy resolution measured with an ⁵⁵Fe source at the same operating point must be below 12%.

The chambers are transferred onto a 2D scanning device. The gas tightness is evaluated by flushing the chamber while monitoring the oxygen content. The voltage settings for an effective gain of 2000 are determined for each GEM stack. These settings are used in the following tests. The energy resolution is measured for each GEM stack at one point with an ⁵⁵Fe source. The resolution is determined by a Gaussian fit to the spectrum. Gain uniformity and ion backflow are measured with x-ray irradiation at each point using the 2D scanner. A

chamber passes the test if the gain uniformity is better than 20%. An example of the ion backflow is shown in Fig. 1.

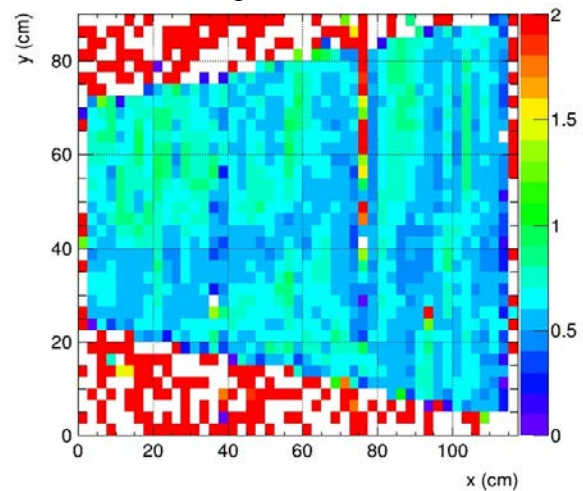


Figure 1: Two-dimensional scan of the ion backflow showing the uniformity of the chamber OROC/6.

Each solder joint of the high voltage connections and the GEM foils is irradiated for 15 minutes to check for possible defects which may cause discharges. After the 2D scans, the chamber load exceeding the anticipated LHC Run 3 and Run 4 conditions is simulated in a shielding box. During this six-hour-long full area irradiation the chamber is monitored for possible discharges. Subsequently the leakage current for each GEM is measured to be able to exclude any possible short circuits. If a chamber passes all the tests, it is moved into a transportation box in which it will be sent to CERN.

The work at the GSI detector lab is progressing well. The first two chambers were already shipped to CERN. The final assembly of the TPC will take place in 2019.

Work supported by BMBF and GSI.

References

- [1] The ALICE Collaboration, “Upgrade of the ALICE Time Projection Chamber”, CERN,

October 2013,
<https://cds.cern.ch/record/1622286>

Read-out electronics for the ALICE TPC upgrade

C. Lippmann¹ and the ALICE collaboration

¹GSI, Darmstadt, Germany

The front-end electronics for the upgrade of the ALICE Time Projection Chamber (TPC) is based on the 32-channel SAMPA ASIC and a radiation-hard data and control link (CERN GBT). The SAMPA ASIC incorporates for each channel a charge-sensitive amplifier, a shaper, and a 10-bit ADC. The TPC uses the SAMPA (5 per Front-End Card, FEC) in direct-serialization mode, where all ADC values are sent via electrical links to the GBTx multiplexer ASIC (2 per FEC) and through the optical read-out links without compression. In this way, the data can be corrected for the Common Mode Effect in the FPGA-based read-out card, the ALICE Common Readout Unit (CRU), with high precision. The Common Mode Effect is a systematic, common baseline shift expected at high occupancies.

Beamtest results

A pre-production Inner Readout Chamber (IROC) has been tested together with 6 prototype versions of the TPC FEC with SAMPA chips of version 'v2' at the CERN Proton Synchrotron with electrons and pions at 1 to 6 GeV/c. Since CRUs were not yet available the Read-Out Receiver Card (RORC) of the current ALICE experiment was fitted with a custom firmware (T-RORC) implementing the 12 bi-directional GBT links necessary for communicating with the 6 FECs.

The SAMPAs on the 6 FECs are synchronised with dedicated control signals. They synchronously sample the detector signals on 960 channels. Triggers from the beam scintillators are received on the T-RORC and open a time window of 0.1 ms length, where the ADC data are stored to disk.

The particle identification achieved at 1 GeV/c is shown in Fig. 1. The separation power is compatible with the value expected at this short track length (63 pad rows). For a full TPC sector the deposited charge information from 152 pad rows will be used, and the separation power will improve accordingly.

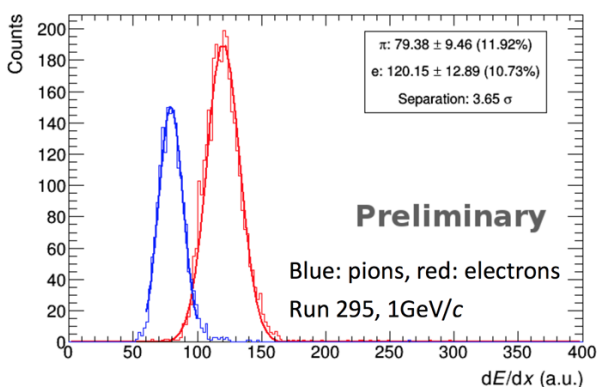


Figure 1: Particle separation power (electrons and pions) measured with a TPC pre-production IROC.

The read-out system was running stable for the full beam time over many days. No issues with synchronisa-

tion between the SAMPAs have been seen. During and after the beam test the data decoded, reconstructed and analysed with software based on the official ALICE online-offline package.

Noise results

The TPC FEC connects to the detector via flexible signal cables (in order to decouple the weight from the FEE from the read-out chambers and drift field cage). The Printed Circuit Board (PCB) for the final version is based on rigid flex technology where the flexible cables are realized as one layer of the PCB (see Fig. 2).

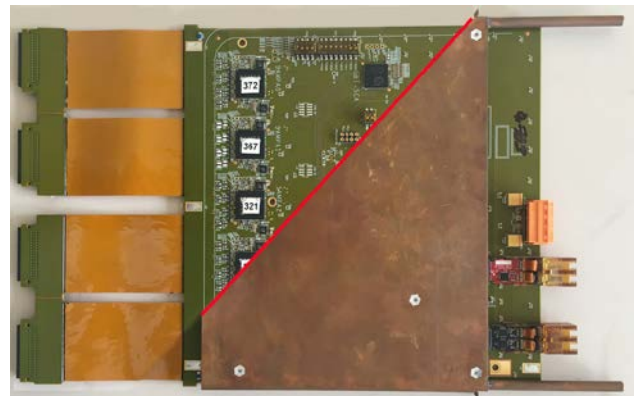


Figure 2: Overlay of 2 images showing a TPC Front-End Card (FEC) with and without its copper cooling envelope. The 4 flexible signal cables, the input protection network and the SAMPA ASICs are visible on the left, the power and optical connectors on the right.

FECs of this revision ('1a') and equipped with the different versions of the SAMPA (v2, v3 and v4) have been tested on the IROC after the beamtest. A noise distribution for 6 FECs is shown in Fig. 3. The mean noise in this particular detector region is 0.93 LSB. The targeted noise value is 1 LSB, corresponding to an equivalent noise charge (ENC) of 670 electrons.

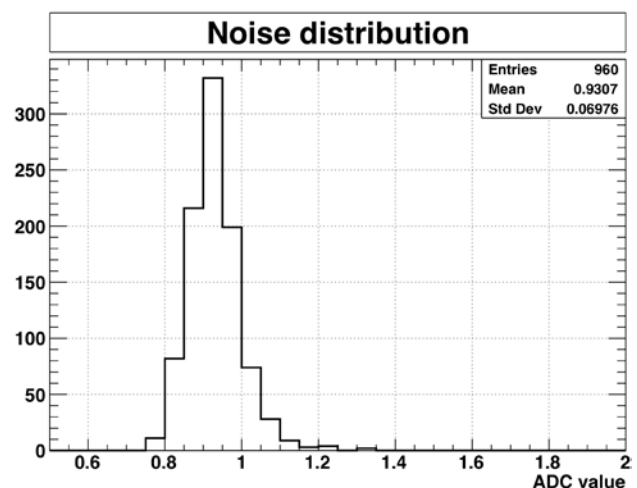


Figure 3: Noise distribution on 960 channels using 6 revision '1a' FECs.

The revision '1a' of the FEC with SAMPA v4 will go into production. The SAMPA production readiness review (PRR) was successfully held on 20 February 2018. The PRR for the TPC FEC is planned for Spring 2018.

*Work supported by BMBF and GSI.

Nuclear modification factors in Xe-Xe collisions measured with ALICE*

J. Gronefeld¹ for the ALICE collaboration

¹GSI, Darmstadt

The suppression of charged particle yields in heavy-ion collision compared to a superposition of independent nucleon-nucleon collisions at RHIC was one of the first indications of the creation of a deconfined medium [1, 2]. This observation is related to parton energy loss in the hot and dense QCD matter created in the collision of heavy ions, leading to a modification of transverse-momentum (p_T) distributions of the resulting particles, as initially suggested by Bjorken in 1982 [3].

Results from ALICE [4, 5] show that hadron yields at high p_T in central Pb–Pb collisions at LHC are suppressed even stronger than at RHIC, indicating a hotter and denser medium.

The suppression is quantified in terms of the nuclear modification factor:

$$R_{AA} = \frac{dN_{AA}/dp_T}{\langle T_{AA} \rangle d\sigma_{pp}/dp_T}$$

Here, dN_{AA}/dp_T represents the p_T -differential charged-particle yield in nucleus-nucleus (AA) collisions, while $d\sigma_{pp}/dp_T$ stands for the p_T -differential cross section in proton-proton (pp) collisions. The average nuclear overlap function $\langle T_{AA} \rangle$ is determined by Glauber Monte-Carlo calculations for each class of centrality. In absence of medium effects, the nuclear modification factor will be equal to unity, while $R_{AA} < 1$ indicates a suppression of charged-particle yields.

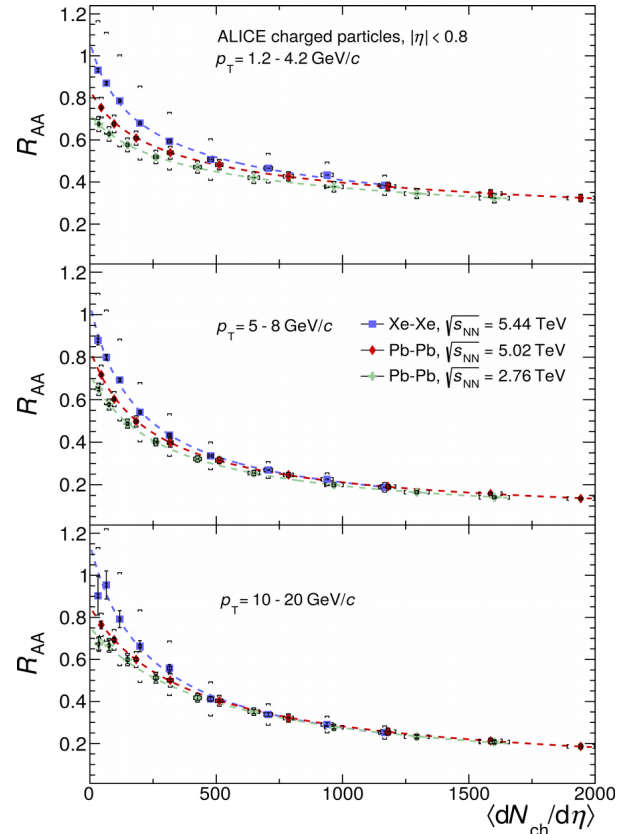
To obtain the primary charged-particle yield as a function of p_T , corrections are made for tracking efficiency and acceptance and for contamination by secondary particles. These correction factors are obtained from Monte-Carlo simulations that are reweighted to account for differences in the particle composition of event generators and the data. In addition the distribution is corrected for p_T resolution.

The charged particle nuclear modification factor for Xe-Xe and Pb-Pb collisions at two different center-of-mass energies is shown as a function of the charged particle multiplicity per unit of rapidity for three ranges in p_T . All systems exhibit a similar trend, showing an increase in

suppression for events with a increased charged particle production.

For high charged particle densities we observe the same R_{AA} for all collision systems and for all energies at high p_T where parton energy loss is believed to play a dominant role (lower panel). This shows that a deconfined medium is created in heavy-ion collisions that exceeds a charged particle density of 400 per unit of rapidity independently of the collision system.

At low p_T (top panel) a energy dependence of the R_{AA} is observed, which is attributed to the increased particle production with higher collision energy.



The charged particle R_{AA} as a function of charged particle density.

[1] PHENIX Collaboration, Phys. Rev. Lett. 88, (2002) 022301.

[2] STAR Collaboration, Phys. Rev. Lett. 89, (2002) 202301.

[3] J. Bjorken, Preprint FERMILAB-PUB-82-059-THY (1982).

[4] ALICE Collaboration, Phys. Lett. B 746, (2015).

[5] ALICE Collaboration, arXiv: 1802.09145 (2018).

* Work supported by GSI, TU Darmstadt and HGS-HIRE

Measurement of ^3He elliptic flow in Pb-Pb collisions with ALICE at the LHC

A. Caliva¹, the ALICE collaboration

¹GSI, Darmstadt, Germany

The elliptic flow coefficient (v_2) of (anti-) ^3He is measured as a function of p_T in Pb-Pb collisions at $\sqrt{s_{NN}} = 5.02$ TeV for different centrality ranges using the Event Plane (EP) method [1].

This measurement provides an important contribution to the understanding of collectivity effects for loosely bound nuclear systems, complementing the picture obtained from the v_2 of (anti-)deuterons [2] and (anti-)protons [3], and puts additional constraints to the coalescence approach and other hadronization models that describe the elliptic flow of light (anti-)nuclei in heavy-ion collisions.

Analysis strategy

In Pb-Pb collisions with non-zero impact parameter, the hot and dense partonic matter is created with an initial spatial asymmetry with respect to the reaction plane, defined by the impact parameter and the beam direction.

This initial geometrical anisotropy produces a non-uniform azimuthal distribution of particles with respect to the reaction plane, due to the different pressure gradients “in-plane” and “out-of-plane”.

The elliptic flow coefficient (v_2) is defined as the asymmetry between the numbers of particles emitted in-plane and out-of-plane:

$$v_2 = \frac{\pi}{2R_2} \frac{N_{\text{in-plane}}(\rho_T) - N_{\text{out-of-plane}}(\rho_T)}{N_{\text{in-plane}}(\rho_T) + N_{\text{out-of-plane}}(\rho_T)}$$

The centrality of the collision is determined from the charged particle multiplicity measured by two forward detectors (V0A and V0C).

Pileup rejection is applied to select single Pb-Pb collisions and all events are required to have a reconstructed vertex within 10 cm from the geometric centre of the ALICE experiment in order to ensure a uniform response of the detectors in the central barrel.

All reconstructed tracks are required to fulfil a set of track quality criteria. The ^3He candidates are identified by requiring that their specific energy loss dE/dx in the TPC is within 3σ from the expected mean for ^3He calculated from the

Bethe-Bloch formula, being σ the resolution in the dE/dx measurement.

The contribution from secondary ^3He produced by spallation in the detector material is suppressed by selecting tracks with transverse distance-to-closest approach (DCA) to the primary vertex smaller than 0.1 cm.

The systematic uncertainties due to tracking, particle identification, occupancy effects in the TPC, event selection and feed-down from weak decays of hyper-triton, are in the range 6-8%.

Results

The elliptic flow of ^3He measured in Pb-Pb collisions at 5.02 TeV, shown in Fig.1, has a clear centrality dependence and a slower rise with p_T compared to other particle species due to the larger mass of ^3He [3].

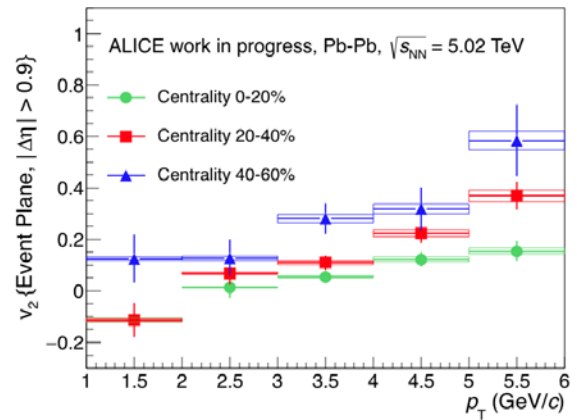


Figure 1: Elliptic flow coefficient (v_2) of ^3He as a function of p_T measured in Pb-Pb collisions at $\sqrt{s_{NN}} = 5.02$ TeV for different centrality classes.

References

- [1] A. Bilandzic et al., Phys. Rev. C 83, 014909 (2011).
- [2] S. Acharya et al., The ALICE Collaboration, Eur. Phys. J. C77, 658 (2017).
- [3] B. Abelev et al., The ALICE Collaboration, JHEP 06, 190 (2015).

Experiment collaboration: CERN-ALICE
Accelerator infrastructure: CERN-LHC

Work supported by GSI

Optimization of the HV scheme for GEM-based detectors

L. Lautner^{1,2}, P. Gasik^{1,2}, L. Fabbietti^{1,2} and the ALICE TPC collaboration

¹Physik Department E62, TU München, 85748 Garching, Germany; ²Excellence Cluster 'Origin and Structure of the Universe', 85748 Garching, Germany

Gas Electron Multiplier (GEM) [1] - based detectors are widely used in many experiments (COMPASS, LHCb, TOTEM) and future upgrades (ALICE, CMS). Electrical discharges that may occur during operation of those detectors can damage them permanently in form of increased leakage currents or electric short circuits that render the detector effectively blind. Initial discharges, caused by high charge densities obtained in a single GEM hole [2] may trigger a propagated (secondary) discharge between two GEMs in a stack or between the last GEM and the readout anode. The latter is especially dangerous - as the front-end electronics can be severely affected by high energy released in a discharge event. The behaviour of the electric field in the gap between GEM foils or a GEM foil and the readout anode after an initial spark cannot explain the appearance of the propagated discharges whose nature is still not fully understood. However, the thorough optimization of the HV scheme in terms of its RC characteristics allows to mitigate (or even avoid) the appearance of these potentially harmful events. In this report we present our measurements on the influence of the RC components on the propagated discharge probability. The study has been conducted with a single $10 \times 10 \text{ cm}^2$ GEM foil in Ar-CO₂ (90-10) and Ne-CO₂-N₂ (90-10-5) mounted at a 2 mm distance to the readout anode (induction gap) and a drift gap, between the cathode and the GEM, of 19.5 mm. A mixed (²³⁹Pu, ²⁴¹Am, ²⁴⁴Cm) source is placed on top of the cathode, emitting alpha particles perpendicular to the GEM. The voltage difference across the GEM was set sufficiently high to increase the primary discharge probability.

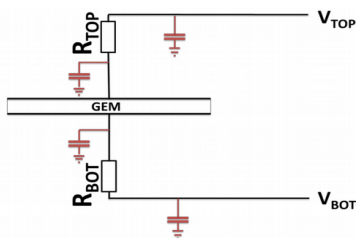


Figure 1: HV scheme of the system with all considered RC elements

Figure 1 presents the RC elements of the HV scheme used in the measurements. Each cable in the system introduces a parasitic capacitance marked in red in the scheme. R_{TOP} and R_{BOT} are the decoupling resistors installed on the top and the bottom side of the GEM, respectively. Particular

attention should be paid to R_{BOT} as it has a significant influence on the secondary discharge probability as shown in Fig. 2.

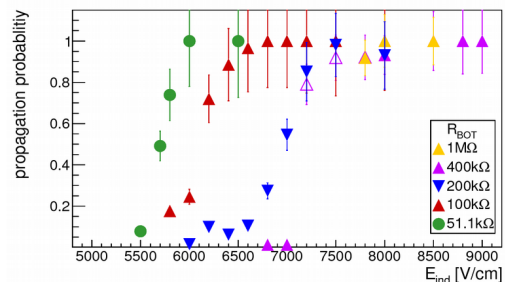


Figure 2: Secondary discharge probability for different values of the decoupling resistor R_{BOT} as a function of the induction field in Ar-CO₂ (90-10)

A large resistance on the GEM bottom electrode increases the potential of that electrode after a primary discharge and thus also the induction field which should make propagation more likely. In contrary, however, the measured onset of the propagated discharges increases with the increasing value of the induction field. This points to a development of a current in the induction gap which, as a consequence, induces a current across the R_{BOT} resistor. The latter results in a potential drop (thus the decrease of the induction field) and quenching of a propagated discharge. Therefore, a clear recommendation for $R_{BOT} > 0$ can be given. In the course of this study, a set of recommendations for the stable operation of GEM detectors has been derived. The Cable length between decoupling resistors and GEM electrodes should be minimized as additional capacitances may keep E_{IND} high after primary discharges. As the cable length between the power supply and the decoupling resistors does not influence the propagation probability for sufficiently large values of R_{BOT} and R_{TOP} , those can be freely chosen. For R_{BOT} , a value greater than 100 k Ω has been proven acceptable. The measurements presented in this report may serve as a baseline for the HV scheme optimization of multi-GEM based detectors.

References

- [1] F. Sauli, NIM A 386 (1997) 531-534
- [2] P. Gasik, A. Mathis & L. Fabbietti, NIM A 870 (2017) 116-122

Experiment beamline: none

Experiment collaboration: CERN-ALICE

Experiment proposal: none

Accelerator infrastructure: none

PSP codes: none

Grants: GSI F&E TMLFRG1316 CBM-RICH

Strategic university co-operation with: none

dE/dx resolution studies of a pre-production read-out chamber with GEMs for the ALICE TPC

T. Klemenz¹, P. Gasik¹, A. Mathis¹, H. Schulte², J. Wiechula²

¹Physik Department E62, Technische Universität München, Germany; ²IKF, Goethe Universität Frankfurt am Main, Germany

The ALICE Collaboration is planning a major upgrade of its central barrel detectors to be able to cope with the increased LHC luminosity beyond 2020 [1]. In order to record at an increased interaction rate of up to 50 kHz in Pb-Pb collisions, the TPC will be operated in an ungated mode with continuous read-out [2]. This demands for a replacement of the currently employed gated Multi-Wire Proportional Chambers by GEM-based (Gas Electron Multiplier) read-out chambers without compromising the performance, in particular in terms of particle identification capabilities via the measurement of the specific energy loss. A stack of 4 GEMs, where two large pitch foils are sandwiched between two standard pitch foils, has proven to meet the requirements when powered with a proper High voltage (HV) configuration. These are an ion back flow (IB) $< 1\%$ and an energy resolution for a ^{55}Fe source ($\sigma(^{55}\text{Fe})$) $< 12\%$. The increase in interaction rate and the requirements of a continuous read-out not only demand for significant modifications of the read-out chambers, but also the front-end cards and the corresponding software framework.

To validate the performance of a 4-GEM Inner Read-Out Chamber (IROC) from the pre-production phase of the project, the dE/dx resolution was evaluated with a beam of electrons and pions at the Proton Synchrotron at CERN. The detector was equipped with the newly developed front-end electronics based on the SAMPAs ASICs [3], sampling the signal with 5 MHz. Throughout the measurements, 11 HV configurations, corresponding to different values of the local energy resolution and IB , were used to power the IROC. The online and offline data analysis was conducted with O^2 , the new software framework for reconstruction, simulation and analysis in ALICE.

For the data analysis, only events with single tracks were selected in order to make use of the particle identification provided by a threshold Cherenkov counter as a reference. Local gain variations in the GEM stack and channel-by-channel variations of the front-end electronics may cause variations of the gain. These were measured and corrected for on a pad-by-pad level. With a width of 6.3% these gain variations are very well within the specifications of $< 10\%$. At 1 GeV/c, a dE/dx resolution for pions (11.92%) and electrons (10.73%) as well as the corresponding separation power (3.65 σ), defined as

$$S_{AB} = \frac{|\langle dE/dx \rangle_A - \langle dE/dx \rangle_B|}{0.5(\sigma(dE/dx)_A + \sigma(dE/dx)_B)} \quad (1)$$

for two particle species A and B , is obtained.

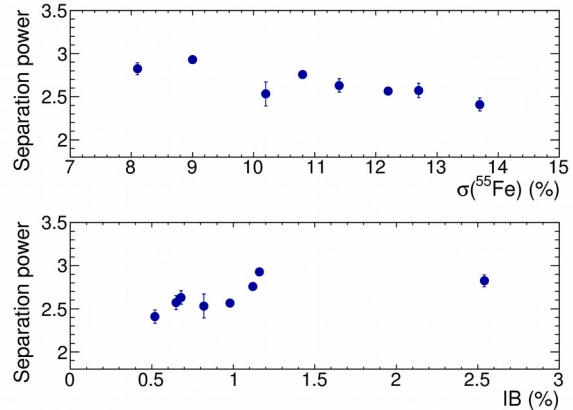


Figure 1: Separation power of electrons and pions as a function of ^{55}Fe resolution (top) and ion back flow (bottom) at a beam momentum of 2 GeV/c

In Fig. 1 the separation power as a function of the ^{55}Fe resolution (top) and the ion back flow (bottom) is shown. The data points represent different HV configurations. One can see that the separation power has only a shallow dependency on those parameters and therefore the separation power does not set any tight constraints on the choice of the final HV configuration for the IROC.

The new read-out system for the TPC upgrade has been tested at the CERN Proton Synchrotron. The read-out chamber, front-end electronics and software framework all work as intended. Currently, the project is in the final production phase. All read-out chambers are scheduled to be assembled until 2019, when the LS2 is supposed to start. The installation and commissioning of the read-out chambers will last until the end of 2020.

References

- [1] B.Abelev et al. [ALICE Collaboration], “Upgrade of the ALICE Experiment: Letter of Intent”, CERN-LHCC-2012-012 (2012), <https://cds.cern.ch/record/1475243>
- [2] B.Abelev et al. [ALICE Collaboration], “Technical Design Report for the Upgrade of the ALICE Time Projection Chamber”, CERN-LHCC-2013-020 (2014), <https://cds.cern.ch/record/1622286>
- [3] S.H.I. Barboza et al., SAMPAs chip: a new ASIC for the ALICE TPC and MCH upgrades, 2016 JINST 11 C02088.

Grants: Excellenzcluster Universe, Origin and Structure of the Universe DFG EClust 153; BMBF ALICE: „Verbundprojekt 05P2015”

Systematic studies of correlations between different order flow harmonics in Pb-Pb collisions at $\sqrt{s_{NN}} = 2.76$ TeV

A. Bilandzic^{1,2}, L. Fabbietti^{1,2}, and the ALICE Collaboration

¹Physik Department E62, Technische Universität München, 85748 Garching, Germany; ²Excellence Cluster ‘Origin and Structure of the Universe’, 85748 Garching, Germany

Systematic studies, comprising the centrality dependence of correlations between the higher order harmonics (the quadrangular v_4 and pentagonal v_5 flow) and the lower order harmonics (the elliptic v_2 and triangular v_3 flow), as well as their transverse momentum dependences, have been recently measured by the ALICE Collaboration, using new flow observables dubbed Symmetric Cumulants. These results provide further constraints on the properties of quark-gluon plasma produced in ultra-relativistic heavy-ion collisions.

Introduction

The main emphasis of the ultrarelativistic heavy-ion collision programs at the Relativistic Heavy Ion Collider (RHIC) and the Large Hadron Collider (LHC) is to study the deconfined phase of strongly interacting nuclear matter, the quark-gluon plasma (QGP). Difference in pressure gradients and the interactions among matter constituents produced in the spatially anisotropic overlap region of the two colliding nuclei result in anisotropic transverse flow in the momentum space. The large values of measured flow harmonics demonstrated that the shear viscosity to the entropy density ratio (η/s) of the QGP in heavy-ion collisions at RHIC and LHC energies is close to a universal lower bound $1/4\pi$ [1].

New constraints on η/s of QGP and on initial conditions in heavy-ion collisions

The newly developed flow observables, Symmetric Cumulants (SC), have provided the first experimental constraints on the temperature dependence of η/s of the QGP produced in heavy-ion collisions [2,3]. In these measurements only the centrality dependence of few lower order SC observables have been reported. The next step in this direction came with the recent measurement of centrality dependence of higher order SC observables and of their transverse momentum dependence [4].

The comparisons to theoretical models show that all the models with large η/s , regardless of the initial conditions, fail to describe the centrality dependence of higher order correlations. Based on the tested model parameters, the data favor small η/s values and the initial conditions obtained from the AMPT model [4].

When it comes to the differential measurements, it was found that SC observables exhibit moderate p_T dependence in midcentral collisions. This might be an indication

of possible viscous corrections to the equilibrium distribution at hadronic freeze-out [4].

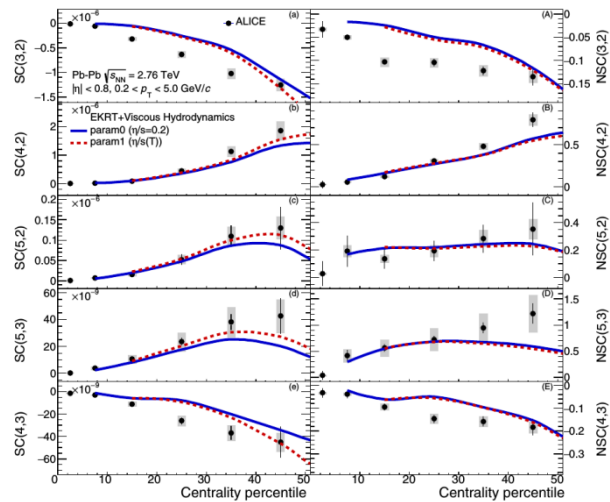


Figure 1: The centrality dependence of SC (left) and normalized SC observables (right) in Pb-Pb collisions at $\sqrt{s_{NN}} = 2.76$ TeV. Results are compared to the event-by-event EKRT+viscous hydrodynamic calculations [5]. The lines are hydrodynamic predictions with two different parametrizations for temperature dependence of η/s .

The calculations for the two sets of parameters which describe the lower order harmonic correlations best are compared to the data in Fig. 1.

Together with the measurements of individual harmonics, these new results for SC observables can be used to further optimize model parameters and put better constraints on the initial conditions and the transport properties of nuclear matter in ultrarelativistic heavy-ion collisions.

References

- [1] P. Kovtun, D. T. Son, A. O. Starinets, Phys. Rev. Lett. 94 (2005) 111601.
- [2] A. Bilandzic et al, Phys. Rev. C 89, 064904 (2014).
- [3] ALICE Collaboration, Phys. Rev. Lett. 117, 182301 (2016).
- [4] ALICE Collaboration, Phys. Rev. C 97, 024906 (2018).
- [5] H. Niemi, K. J. Eskola, and R. Paatelainen, Phys. Rev. C 93, 024907 (2016).

Correction for secondary particles contamination in the charged particle yield measurement in Xe-Xe collisions by ALICE*

M. Habib for the ALICE collaboration
TU Darmstadt and GSI

Introduction

During the LHC operation in 2017 with Xe beams the ALICE experiment has recorded a sample of Xe-Xe collisions with a energy (per nucleon pair, $\sqrt{s_{NN}}$) of 5.44 TeV. A measurement of the primary charged particle transverse momentum (p_T) yield for this collision system is ongoing [1]. The measurement requires precise knowledge about the contamination by particles originating from interaction with the detector material or secondary decays with a lifetime $\tau > 1$ cm/c.

This contamination is usually determined from Monte Carlo (MC) simulations. However, most of the models under predicts the production of secondaries from weak decays. To correct for this phenomena a data driven method based on template fits to the distance to closest approach (DCA), defined as the smallest distance between particle trajectory and the collision vertex, is applied.

Method

Using a MC sample we construct DCA templates for primaries, secondaries originating from decays and interaction with the detector material. The DCA distributions generated with MC have a well known and distinguishable shapes which are shown in the Fig. 1 (upper panel).

A linear combination of the templates can describe the reconstructed data while it gives access to the composition of the measured data sample. However non-physical results were observed showing a larger contribution of secondaries from material than from decay products, which originates due to the fit procedure. To overcome this problem, we assume the relative amount of secondaries form material to be well described in MC and redo the template fit fixing its fraction to the MC prediction. The fit result still describes the data while showing the expected trend. The scaled MC DCA distributions and the ratio of the fit to the measurement are shown in the Fig.1.

Systematic Uncertainty

The ratio deviates from unity by less than 5 %, which is used to assign a corresponding systematic uncertainty on the fit quality.

A second systematic uncertainty is estimated from the fit with two templates only distinguishing between secondaries and primaries. The comparison to the standard method leads to an additional relative uncertainty of roughly 10 % on the reweighting factor.

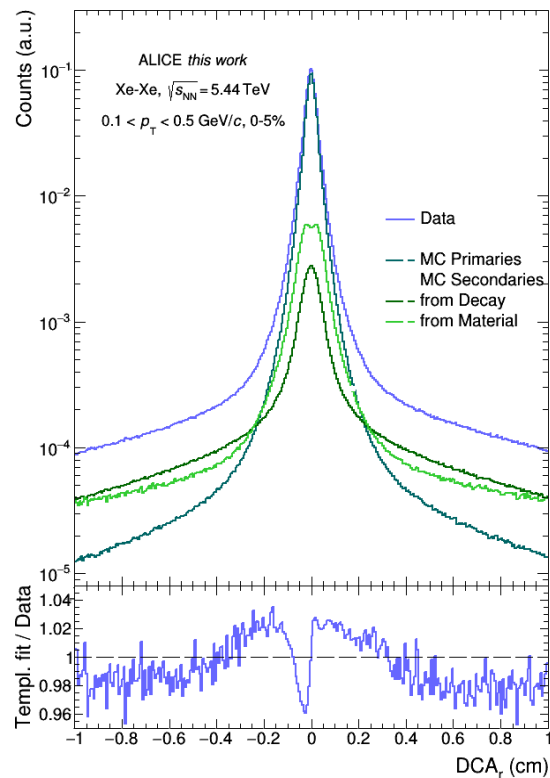


Figure 1: DCA distribution for data and three different MC templates (primaries, secondaries from decay and material) and the ratio of the fit to data.

Result

The fit results show that the secondary particles in the MC are underestimated by 20 - 60 %.

A corresponding reweighting factor is introduced to rescale the secondaries contribution for the primary charged particle yield measurement.

This data driven correction has a significant effect in the small p_T (< 1 GeV) region, while overall having a relative small uncertainty below 3 %.

References

- [1] J. Gronefeld, GSI Scientific Report 2017, contribution 112

* Work supported by GSI, TU Darmstadt and HGS-HIRE

Low-mass dielectron production in Pb-Pb collisions at $\sqrt{s_{NN}} = 5.02$ TeV with ALICE

C. Klein¹ and the ALICE Collaboration

¹IKF, Goethe Universität, Frankfurt, Germany

The ALICE experiment at the CERN-LHC was designed to understand the properties of the strongly interacting quark-gluon plasma (QGP) produced in ultrarelativistic heavy-ion collisions. The production of electron-positron pairs (dielectrons) demonstrated to probe the QGP. Dielectrons only interact electromagnetically and are therefore not affected by the strong force in the hot and dense QGP matter. They are produced in all stages of the collision and therefore give access to the complete spacetime evolution of the system. Whereas proton-lead collisions help to disentangle cold- from hot-medium effects, the dielectron measurement in proton-proton collisions serves as a baseline. With dielectron measurements in lead-lead collisions one can extract directly the temperature of the QGP and can investigate in-medium modifications of the ρ -meson which are associated to a predicted chiral-symmetry restoration [1].

The data set in this study was recorded in 2015 during LHC Run 2 and consists of approximately 84 million events in the centrality class of 0-80% measured in the ALICE central barrel at a center of mass energy of $\sqrt{s_{NN}} = 5.02$ TeV. Electron and positron identification is based on their specific energy loss in the Inner Tracking System (ITS) and in the Time Projection Chamber (TPC). Additionally, the Time Of Flight (TOF) detector helps to reject heavier hadrons. This identification scheme results in a high electron identification efficiency while rejecting most of the hadronic contamination.

To extract dielectron spectra, in every event electrons and positrons are paired forming the so-called unlike-sign spectrum (ULS). The ULS consists of the dielectron signal and additional correlated and combinatorial background. To estimate this background, in each event like-sign pairs are created to form the like-sign spectrum (LS). The dielectron signal is then obtained by subtracting LS from ULS.

Due to a very low signal to background ratio, efficient background rejection is crucial. The major contribution to the combinatorial background originates from real-photon conversions in the detector material and in the beam pipe around the collision vertex. Real-photon conversions dominate at very low invariant masses $m_{ee} < 0.02$ GeV/c² of the signal spectrum, see Fig. 1.

Since photons have zero mass, the electron and positron from a photon conversion are emitted in the same direction. This property is used in two different ways. The first conversion rejection method is exploiting the fact that dielectrons with zero opening angle are very close to each other in the detector. Those two tracks are not distinguishable in a given silicon layer of the ITS: they share an ITS cluster. Selecting only tracks with zero shared clusters in the ITS leads to a reduction of conversion dielec-

Work supported by: BMBF and Helmholtz Association

trons by a factor of 98.5% while keeping 68% of the dielectron signal.

The second method takes advantage of the pair orientation of conversion dielectrons ϕ_V relative to the magnetic field which is given only by the magnetic field of the ALICE solenoid magnet. This property allows to separate them from dielectrons from hadronic decays where the pair orientation is random. While charge-ordered conversion pairs show a peak at higher ϕ_V , signal pairs have no angular correlation. Remaining conversion pairs can be rejected by choosing only pairs with $\phi_V < 2$ and correcting for the cut. These two conversion rejection methods, higher statistics and better understanding of the detector lead to an improved performance of the Pb-Pb dielectron analysis compared to the Run 2 analysis at $\sqrt{s_{NN}} = 2.76$ TeV [2].

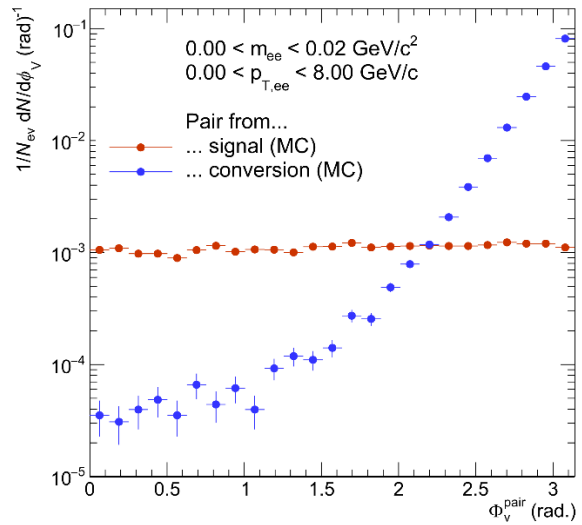


Figure 1: Dielectron signal pairs (red) and conversion pairs (blue) at very low mass $m_{ee} < 0.02$ GeV/c². Selecting tracks with zero shared ITS clusters reduces the conversion contribution by 98.5% while keeping 68% of the total signal. A subsequent selection on pairs with $\phi_V < 2$ reduces remaining contribution by conversions pairs.

References

- [1] Rapp, Chanfrey, Wambach. (1995). Medium Modifications of the Rho Meson at CERN/SPS Energies. *Phys.Rev.Lett.* 76 (1996) 368-371
- [2] Calivà, Alberto. (2017). Measurement of dielectrons in pp, p-Pb and Pb-Pb collisions with ALICE at the LHC. *Journal of Physics: Conference Series.* 779. 012052.10.1088/1742-6596/779/1/012052

Proton-proton reference spectrum at $\sqrt{s} = 5.44$ TeV

E. Perez Lezama¹ for the ALICE collaboration

¹GSI, Darmstadt, Germany

Particle production at high energies is often described as a result of the interplay of perturbative (hard) and non-perturbative (soft) QCD processes. Therefore, the measurements of transverse momentum spectra in pp collisions are important to provide a baseline for calculations in perturbative QCD and constraints for a better tuning of models and event generators. In addition, they constitute a valuable reference to study nuclear effects in nucleus-nucleus and proton-nucleus collisions, in particular allowing one to measure the nuclear modification factors.

In order to calculate the nuclear modification factor, a pp reference for the same collision energy is required. Since the Xe–Xe data was taken at $\sqrt{s_{NN}} = 5.44$ TeV, and there is no pp measurement available at this energy, we construct the pp reference using measured data at $\sqrt{s} = 2.76$ TeV, $\sqrt{s} = 5.02$ TeV [2] and $\sqrt{s} = 7$ TeV. We have implemented two different methods:

- Scaling the $\sqrt{s} = 5.02$ TeV pp spectrum up using the PYTHIA 8 Monash tune event generator, as shown in equation 1.
- Interpolation between the data at $\sqrt{s} = 5.02$ TeV and $\sqrt{s} = 7$ TeV assuming a power law behaviour as a function of \sqrt{s} .

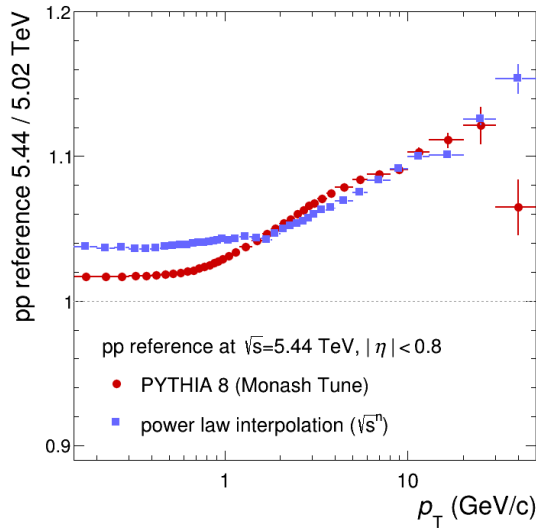
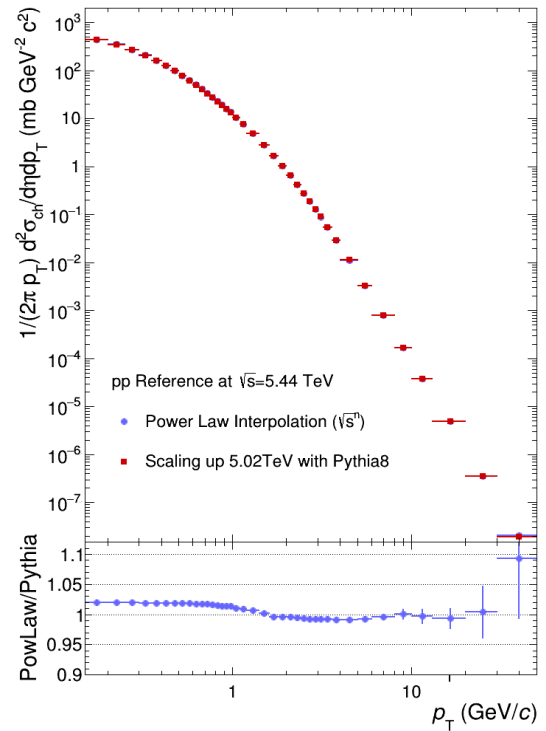


Figure 1: Ratio of generated p_T -differential cross section in pp at $\sqrt{s} = 5.44$ TeV to the measured one at $\sqrt{s} = 5.02$ TeV.

The ratio of the pp reference spectra at $\sqrt{s} = 5.44$ TeV and $\sqrt{s} = 5.02$ TeV from the power-law extrapolation is shown in figure 1 together with results obtained with the alternative method. The systematic uncertainty of the pp reference at $\sqrt{s} = 5.44$ TeV has two contributions which are ad-

ded quadratically. For each p_T interval, we take the systematic uncertainty of the pp references at $\sqrt{s} = 5.02$ TeV and $\sqrt{s} = 7$ TeV and interpolate them by a power-law fit to $\sqrt{s} = 5.44$ TeV. Figure 2 shows the interpolated reference spectrum compared to the reference constructed using PYTHIA-scaling.



$$\frac{d\sigma}{d\eta dp_T} = \frac{\left(\frac{d\sigma}{d\eta dp_T}\right)_{\sqrt{s}=5.02 \text{ TeV}}^{\text{Measured}} \times \left(\frac{d\sigma}{d\eta dp_T}\right)_{\sqrt{s}=5.44 \text{ TeV}}^{\text{MC}}}{\left(\frac{d\sigma}{d\eta dp_T}\right)_{\sqrt{s}=5.44 \text{ TeV}}^{\text{MC}}} \quad (1)$$

Figure 2: p_T -differential cross section in pp at $\sqrt{s} = 5.44$ TeV and the measured one at $\sqrt{s} = 5.02$ TeV. Bottom panel shows the ratio of the two cross sections.

References

- [1] arXiv:1802.09145
- [2] Eur. Phys. J. C 73 (2013) 2662

Production of antiparticles in p-Pb collisions at 5.02 TeV with ALICE

L.Córdova¹, B.Hohlweger¹, L.Fabbietti^{1,2}, for the ALICE collaboration

¹Technische Universität München, Physik Department E62, Garching Germany; ²Excellence Cluster 'Origin and Structure of the Universe', Garching, Germany

Under the assumption that dark matter particles can annihilate to form standard model particles, the indirect search for dark matter looks for these annihilation products. Cosmic-ray particles and antiparticles can often be challenging to detect due to a high background originating from the high-energy cosmic ray propagation through the interstellar medium. Low-energy antideuterons, however, have an ultra-low astrophysical background. The predicted flux of antideuterons originating from the annihilation of various viable dark matter candidates exceeds the background flux by more than two orders of magnitude in the kinetic energy range below 0.25 GeV/n. For that reason, low-energy antideuterons could be a unique probe for indirect searches for dark matter [1].

Hence, for the indirect dark matter search it is important to understand how antideuterons interact with matter. The ALICE detector allows to identify and track antideuterons from its creation in the collision or from decays. Since the ALICE Transition Radiation Detector (TRD) has a high material budget, the interaction probability of antideuterons with this detector can be investigated by analyzing the products with the next detector layer, the ALICE Time Of Flight detector (TOF). The basic principal of the measurement is shown in Figure 1.

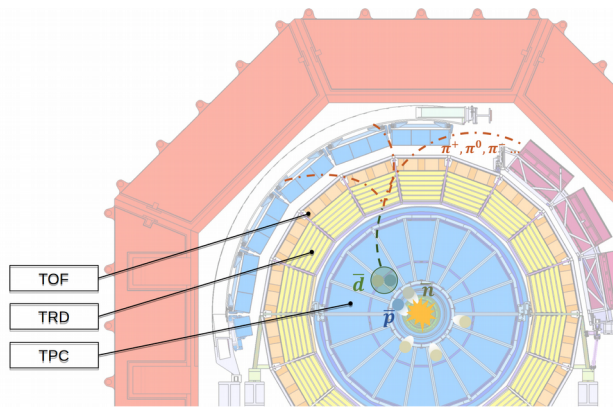


Figure 1: Cross section of the ALICE detector. Schematic representation of an antideuteron that interacts with the TRD material and produces a pion shower, which can be analyzed with the TOF.

In order to have a baseline in the antideuteron analysis, beside (anti-)deuterons, also (anti-)protons are identified in a first step.

During the analysis, a kink at the momentum region $p \sim 1.0$ GeV/c was found in the (anti-) proton spectrum. By looking at the mass hypothesis for the energy loss correction in the ALICE Time Projection Chamber the source of this irregularities was found. In the region $p \sim 1.0$ GeV/c an electron mass was assumed to correct protons and this led to a wrong energy loss correction. The correction was obtained with a fit to the data and implemented to correct the momentum track-by-track.

In a next step the track cuts implemented in the analysis need to be optimized in order to measure the production and extract the absorption cross sections of protons, deuterons and their corresponding antiparticles. Especially the Monte Carlo data of (anti-) deuteron needs further investigation.

The Monte Carlo productions with injected nuclei, which are necessary for the (anti-)deuteron analysis, have an entirely different statistical background than the data and cannot be applied as templates for the yield of primaries and secondaries. At the moment, when calculating the purity of (anti-) deuterons, we get a result of almost 100% in the whole momentum range, which means that there are too many nuclei injected. This is why the yields of the Monte Carlo data first need to be rescaled according to a fit that best describes the experimental sample. Further, it must be considered that scattering data for (anti-) deuterons is very limited but required as an input for the simulation in GEANT for the propagation of (anti-) deuterons through the detector and the resulting detector signals[2].

Finally, the analysis can focus on the conversions of antiparticles when interacting with the TRD material. Since the lower limit of the energy range of identified (anti-) deuterons is given by the surrounding magnetic field, for low energetic (anti-) deuterons an analysis with a lower magnetic field could be done in the future.

References

- [1] T. Aramaki, S. Boggs et al. Review of the theoretical and experimental status of dark matter identification with cosmic-ray antideuterons, *Physics Reports*, 618, 1-37 (2016).
- [2] ALICE Collaboration. Production of light nuclei and anti-nuclei in pp and pb-pb collisions at LHC energies, *Phys. Rev. C* 93, 024917 (2015).

Neutral pion and η meson production in p-Pb and Pb-Pb collisions at the LHC*

A. Marin¹, F. Bock², P. González-Zamora³, Y. Kharlov⁴, L. Leardini⁵, A. Morreale⁶, T. Okubo⁷, A. Passfeld⁸, D. Peresunko⁹, K. Reygers⁵, M. Sas¹⁰, J. Stachel⁵, for the ALICE collaboration

¹GSI Helmholtzzentrum für Schwerionenforschung GmbH, Darmstadt, Germany; ²CERN, Geneva, Switzerland, ³Benemérita Universidad Autónoma de Puebla, Puebla, Mexico, ⁴NRC “Kurchatov institute”-IHEP, Protvino, Russia, ⁵Physikalisches Institut, Ruprecht-Karls-Universität Heidelberg, Heidelberg, Germany, ⁶SUBATECH, IMT Atlantique, Université de Nantes, CNRS-IN2P3, Nantes, France, ⁷Hiroshima University, Hiroshima, Japan, ⁸Institut für Kernphysik, Westfälische-Wilhelms-Universität-Münster, Münster, Germany, ⁹NRC “Kurchatov Institute”, Moscow, Russia ¹⁰Institute for Subatomic Physics of Utrecht University, Utrecht, The Netherlands

Neutral pion and η meson production has been measured in p-Pb collisions at $\sqrt{s_{NN}} = 5.02$ TeV [1] and Pb-Pb collisions $\sqrt{s_{NN}} = 2.76$ TeV [2] with the ALICE experiment at the CERN LHC. The measured η/π^0 ratio deviates from m_T scaling for $p_T < 3$ GeV/c in both systems. At high p_T , a large suppression of the same magnitude for π^0 and η meson production is observed in central Pb-Pb collisions with respect to the scaled pp reference, while the π^0 and η R_{pPb} ratios are consistent with unity above a p_T of 2 GeV/c. These results support the interpretation that high p_T particle suppression in Pb-Pb collisions is due to parton energy loss in the hot QCD medium.

Results

The measurement of neutral pions and η mesons in a broad p_T range in Pb-Pb collisions can provide information on the energy loss mechanisms in the hot QCD medium. Their measurement in p-Pb collisions is needed to disentangle initial and final-state effects.

Photons are reconstructed in ALICE using two complementary techniques: the photon conversion method (PCM), and electromagnetic calorimeters (PHOS and EMCal). Neutral mesons are reconstructed in the two-photon decay channel and additionally in the Dalitz decay channel for the p-Pb system. Neutral pions and η mesons are identified as peaks at their corresponding rest mass in two-photon invariant mass distributions. The invariant differential yields are measured independently in each method and then combined using the Best Linear Unbiased Estimate.

The invariant yields of π^0 , and, for the first time at the LHC, of η mesons have been measured for central and semi-central Pb-Pb collisions at $\sqrt{s_{NN}} = 2.76$ TeV, as well as for non-single diffractive (NSD) p-Pb collisions at $\sqrt{s_{NN}} = 5.02$ TeV up to 20 GeV/c, and compared to different theoretical model predictions [1, 2]. The measured η/π^0 ratio in p-Pb (Fig. 1) and Pb-Pb collisions reaches a plateau value for $p_T > 3$ GeV/c of $0.483 \pm 0.015_{stat} \pm 0.015_{sys}$ and $0.457 \pm 0.013_{stat} \pm 0.018_{sys}$, respectively. For $p_T < 3$ GeV a deviation from m_T scaling is observed in both collisions systems. Decay of heavier resonances into π^0 and presence of radial flow even for the p-Pb system are among the possible explanations. The large radial flow in central Pb-Pb collisions gives rise to the enhancement of the η/π^0 ratio at $p_T \sim 2-4$ GeV/c, as similarly observed for K^\pm/π^\pm . The nuclear modification factor of π^0 or η in Pb-Pb collisions quantifies particle production suppression at high p_T in heavy-ion collisions. For π^0 and η mesons a large suppression factor of $\sim 8-9$ is observed at $p_T = 7$

GeV/c in central 0-10% Pb-Pb collisions (Fig. 2), with increasing trend at higher p_T . The π^0 suppression is stronger than the one observed at lower center-of-mass energies. The π^0 and η R_{pPb} are consistent with unity for $p_T > 2$ GeV/c in p-Pb collisions. These results support the interpretation that π^0 and η meson high p_T suppression in central Pb-Pb collisions is due to parton energy loss in the hot QCD medium.

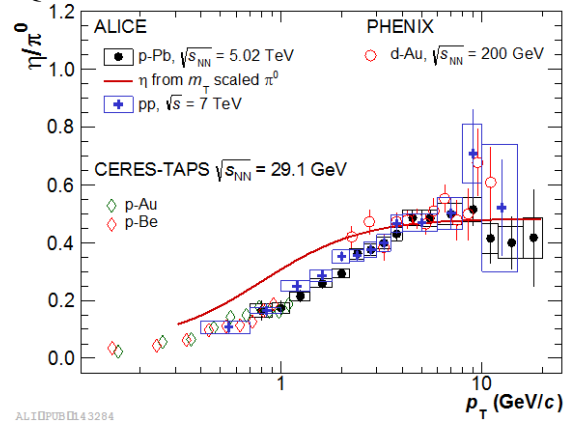


Figure 1: η/π^0 ratio measured in p-Pb collisions compared to m_T scaling and to existing measurements.

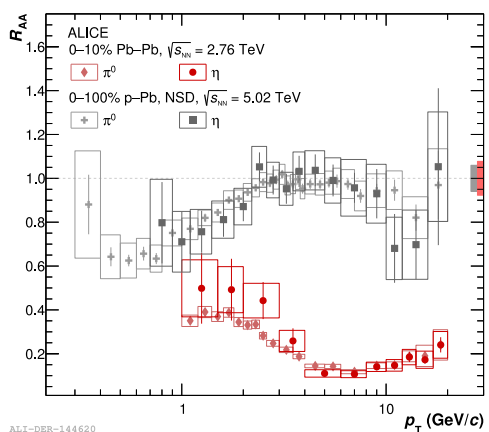


Figure 2: Measured π^0 and η meson R_{AA} in 0-10% central Pb-Pb collisions and in NSD p-Pb collisions.

References

- [1] ALICE Collaboration, S. Acharya *et al.*, “Neutral pion and η meson production in p-Pb collisions at $\sqrt{s_{NN}} = 5.02$ TeV”, arXiv: 1801.07051.
- [2] ALICE Collaboration, S. Acharya *et al.*, “Neutral pion and η meson production at mid-rapidity in Pb-

Pb collisions at $\sqrt{s_{NN}} = 2.76$ TeV”, arXiv: 1803.05490.

*Work supported by BMBF, GSI, and University of Heidelberg

Inclusive and non-prompt J/ψ production in Pb-Pb collisions at $\sqrt{s_{NN}} = 5.02$ TeV measured at mid-rapidity with ALICE

R.T.Jimenez Bustamante^{1,2}, L.Layer^{1,2}, D.Weiser², S.Masciocchi^{1,2}, A.Andronic^{1,3}, I.Arsene⁴,
M.Köhler²,

and the ALICE collaboration

¹GSI, Darmstadt; ²Universität Heidelberg; ³Universität Münster; ⁴University of Oslo

Introduction

Quarkonium and open heavy-flavor production plays a crucial role as a probe of the hot deconfined medium created in heavy ion collisions. The suppression of charmonium production induced by the color screening of quarks was proposed more than 30 years ago as a probe of the formation of the Quark Gluon Plasma (QGP) [1]. At LHC collision energies, the average number of charm-anticharm quark pairs per event exceeds the average number of charm-anticharm quark pairs per event at RHIC by one order of magnitude. Two different approaches [2,3] suggested new production mechanisms playing a role at LHC collision energies, leading to a charmonium enhancement in the most central A-A collisions. The inclusive J/ψ nuclear modification factor R_{AA} measured by ALICE [4,5] at $\sqrt{s_{NN}} = 2.76$ TeV, showed a striking enhancement in central collisions compared to the measurements at lower energies [6,7], supporting the models including (re)generation. The transport and comovers models assume the creation of the charmonium states due to continuous dissociation and regeneration throughout the lifetime of the medium [8,9,10]. On the other hand the statistical hadronization model [11] assumes creation of charmonium at the phase boundary. Due to the increase of the initial number of charm-anticharm pairs relative to the total number of quarks, an increase of the R_{AA} with the collision energy is predicted by the models. The statistics gathered by ALICE during LHC Run 2 measurement at $\sqrt{s_{NN}} = 5.02$ TeV provides essential information for the suppression and regeneration picture.

The determination of the non-prompt J/ψ fraction gives access to the physics of B-hadrons. Since the mass of heavy quarks is large compared to the temperature of the medium, they are produced in the early stage of the collision and thus experience the entire space-time evolution of the system [12]. While there is a strong experimental indication for a thermalization of charm quarks in the medium, beauty quarks are not expected to fully thermalize, since their lifetime is larger than the lifetime of the plasma [13]. Therefore they carry information starting from the beginning of the collision. Experimentally at RHIC and at the LHC a strong

suppression of the nuclear modification factor R_{AA} has been observed [12]. From a theoretical point of view, the large masses of the heavy quarks make the computation of the transport coefficients, which characterize transport properties of the medium, feasible directly from first principle QCD calculations [13]. Measurements of the nuclear modification factor R_{AA} and the flow coefficient v_2 of heavy-flavour hadrons are an essential observable to constrain phenomenological models that build a bridge between experiment and first principle QCD calculations.

Inclusive J/ψ production

The ALICE experiment [14] allows to measure J/ψ mesons at mid-rapidity ($|y| < 0.8$) in the dielectron decay channel. Two main detectors are used for the electron reconstruction. The Inner Tracking System (ITS), consisting of six layers of silicon detectors located around the interaction point, is used for tracking, vertex determination and triggering. The Time Projection Chamber (TPC) is the main tracking detector and is also used for particle identification via the measurement of the specific energy loss in the detector gas (dE/dx). The electrons are identified using the TPC information, and the invariant mass distribution is constructed using opposite sign pairs.

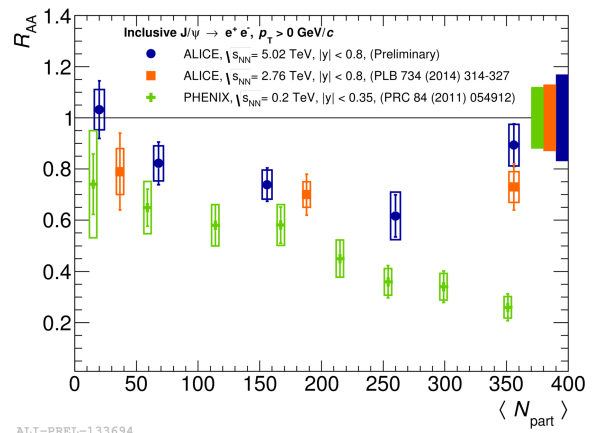


Figure 1: Nuclear modification factor of inclusive J/ψ as a function of centrality at different energies.

The analysis of the inclusive and non-prompt J/ψ production presented here is based on 75 million minimum bias events in Pb-Pb collisions at $\sqrt{s_{NN}} = 5.02$ TeV. This allows to measure the inclusive J/ψ production in 5 different centrality classes: 0-10%, 10-20%, 20-40%, 40-60% and 60-90%.

Figure 1 shows the inclusive R_{AA} at $\sqrt{s_{NN}} = 5.02$ TeV as a function of centrality compared to the ALICE measurement at $\sqrt{s_{NN}} = 2.76$ TeV at mid-rapidity [7]. The centrality dependence is similar at the two energies. However, a slight increase is observed in the most central collisions. Within the uncertainties the results at both energies are compatible. The measurement by PHENIX at $\sqrt{s_{NN}} = 0.2$ TeV [9] clearly shows a stronger suppression of the R_{AA} values in central collisions compared to ALICE measurements.

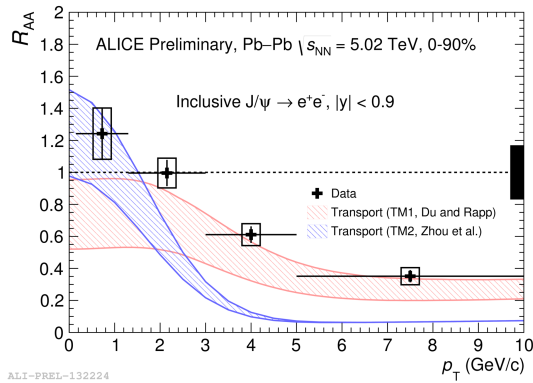


Figure 2: Nuclear modification factor of inclusive J/ψ as a function of transverse momentum.

The inclusive R_{AA} at $\sqrt{s_{NN}} = 5.02$ TeV is also measured as a function of transverse momentum in the centrality classes 0-90%, 0-20%, 20-40% and 40-90%. In figure 2 the results for the 0-90% centrality class is shown. The increase of the R_{AA} towards low momentum is consistent with the (re)generation scenario and in agreement within uncertainties with the model calculations.

Non-prompt J/ψ production

The non-prompt J/ψ fraction coming from the decay of B-hadrons is determined by decomposing the inclusive J/ψ yield into its prompt and non-prompt components via a 2-dimensional log-likelihood fit to the invariant mass and the pseudo-proper decay length of the J/ψ . The distribution of the pseudo-proper decay length of the non-prompt J/ψ mimics the proper decay length of B-hadrons and thus can be used as a discriminative variable. The same selections as for the inclusive J/ψ analysis are applied. Additionally, machine learning techniques are

used to calculate a variable based on the PID and kinematics of the electron candidates in order to enhance the signal-to-background ratio and the significance of the measurement. Figure 3 shows the results for the nuclear modification factor R_{AA} at $\sqrt{s_{NN}} = 5.02$ TeV for the non-prompt J/ψ . The results are shown together with the results of CMS at $\sqrt{s_{NN}} = 2.76$ TeV at mid-rapidity [15] and various models are overlaid [16,17,18]. The measurement of ALICE extends the measurement of CMS towards lower transverse momentum. A strong suppression of the nuclear modification factor is observed for intermediate and high transverse momenta. Qualitatively, the models are in agreement with the measurement.

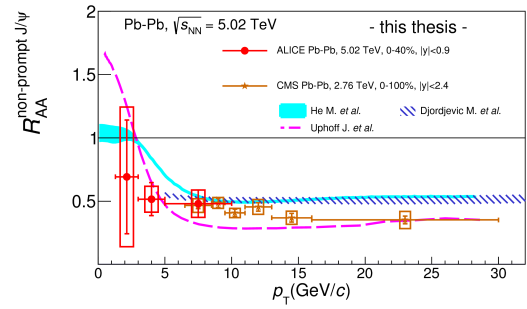


Figure 3: Nuclear modification factor of non-prompt J/ψ as a function of transverse momentum.

References

- [1] T.Matsui, H.Satz, Phys Lett B.178 (1986) 416
- [2] P. Braun-Munzinger, J. Stachel, Phys. Lett. B 490, (2000) 196–202
- [3] R. L. Thews, M. Schroedter, J. Rafelski, Phys. Rev. C 63, (2001) 054905.
- [4] ALICE Coll., Phys.Rev.Lett. 109 (2012) 072301
- [5] ALICE Coll., Phys. Lett. B 734 (2014) 314–327.
- [6] NA 50 Coll., Eur. Phys. J. C 39, 335 (2005)
- [7] PHENIX Coll.Phys. Rev. C 84, 054912 (2011).
- [8] X Zhao, R. Rapp, Nucl. Phys. A 859 (2011) 114–125.
- [9] K. Zhou et al, Phys. Rev. C 89 5, 459 (2014) 054
- [10] E.G. Ferreira, Phys. Lett. B 731 (2014) 57–63
- [11] A.Andronic, P. Braun-Munzinger, J. Stachel, Phys. Lett. B 652 (2007) 259-261
- [12] A. Andronic and others, Eur. Phys. J. C76 (2016)
- [13] Aarts, G. and others, Eur. Phys. J. A53 (2017)
- [14] ALICE Coll., Int. J. Mod. Phys. A 29 (2014) 1430044
- [15] CMS Coll., Eur. Phys. J. C77 (2017)
- [16] Djordjevic, Magdalena and Djordjevic, Marko, Phys. Lett. B734 (2014)
- [17] Uphoff and others, Phys. Lett. B717 (2012)
- [18] He and others, Phys. Lett. B735 (2014)

Stability tests of ALICE TPC GEM chambers at the LHC

C. Garabatos¹, K. Schweda¹, Robert Münzer², Renato Negrao³, and Rainer Renfordt²

¹GSI, Darmstadt, Germany; ²Goethe University, Frankfurt, Germany; ³University of São Paulo, Brazil

The current multi-wire proportional chambers of the ALICE TPC are replaced by new chambers composed of quadruple stacks of GEMs as detectors for the forthcoming LHC Run 3, in 2020.

The production of these 80 (72 plus spares) detectors is ongoing. As ultimate test for the stability of these micro-pattern devices against discharges under the harsh condition of the LHC, a subset of the final detectors are sequentially operated in the ALICE cavern at the LHC itself.

Sets of two detectors (one Inner and one Outer Readout Chamber) are placed close to the LHC beam pipe at about 10 m from the interaction point at the ALICE cavern, where particle densities are about one order of magnitude higher than those expected in the TPC chambers in Run 3 with 50 kHz Pb-Pb collision rate. Figure 1 shows one OROC under the beam pipe at the ALICE experiment.

The detectors are included in the TPC gas circuit and are thus operated with the same gas mixture. They are powered with a HV system which includes the final, cascaded power supplies especially designed for GEM operation, protection resistor networks close to the detector, and a set of high precision, high bandwidth picoammeters. A custom-made Labview application allows for a safe operation of the HV system, including automatic ramping according to the LHC modes, such that the HV is on only when there is no beam or stable beams. The voltages and currents are thus monitored and recorded, potential current excursions analysed, and a tripping mechanism is put in place.

All pads of each readout plane are connected together into a digital oscilloscope, located in the cavern, which is remotely controlled and readout. Thus, the operator can control and monitor the detectors from the surface, since there is no access to the cavern while beams are on the machine.

The HV powering scheme is a crucial aspect for the safe operation of these detectors, since the voltage in each electrode of the GEM stack is closely coupled to the voltages in the neighbouring electrodes. Thus, if a spark in a given place leads to an overvoltage between any two electrodes, further sparking may result into irreversible damage of the GEM foils.

Operation of first prototypes in this manner showed instabilities and damage due precisely to the sub-optimal HV configuration strategy. Further improvements – adequate choice of protection resistor networks, cascading scheme, tripping mechanism, decoupling resistors – lead to success.

Final production chambers were thus exposed to the LHC conditions at forward rapidity under nominal gas and HV conditions without any trips for several weeks of operation. Minor discharges were recorded during this period. Operation included special ALICE tests where the particle rates expected in Run 3 were reproduced in the experiment, which resulted in about one order of magni-

tude higher doses in the forward location of the Upgrade GEM detectors.

Plans for 2018 are to periodically install in the ALICE cavern two sets of detectors with four readout chambers in total – two inner readout chambers and two outer ones-, operate them for several weeks, and then replace them during technical stops or other suitable opportunities, in order to qualify a meaningful subset of the full production.

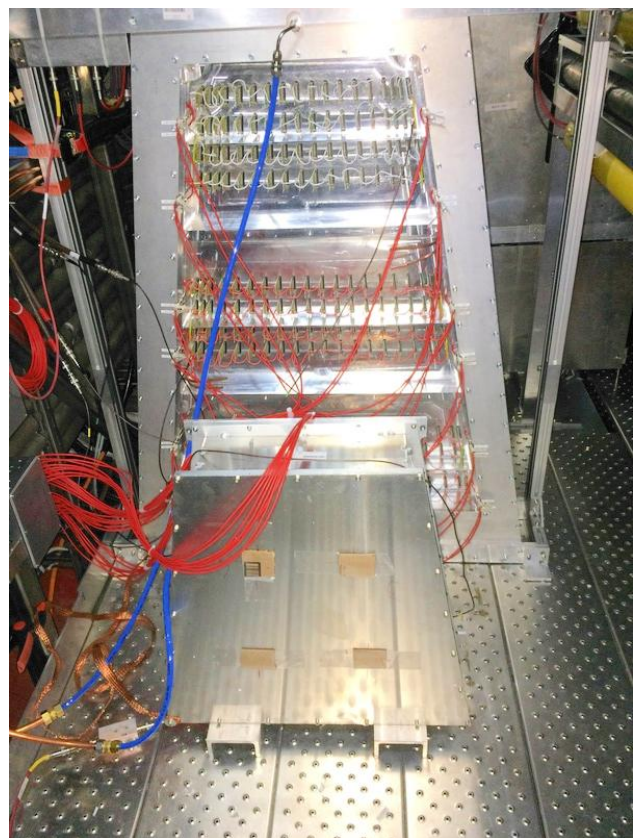


Figure 1: Set of two chambers placed close to the LHC beam pipe in the ALICE cavern ready to be operated with beams.

Experiment collaboration: CERN-ALICE

PSP codes: none

Strategic university co-operation with: Frankfurt-M / Heidelberg / Munich / Bonn / Budapest / Bucharest / Helsinki / New Haven / Oakridge / Detroit

*Work supported by BMBF, GSI.

Report by the GSI-ALICE group

K. Schweda¹, for the ALICE collaboration

¹GSI, Darmstadt, Germany

ALICE is currently engaged in the Run-2 period of the LHC operation at CERN that started in 2015. Collisions of lead nuclei (Pb) at the highest energy ever reached in the laboratory were recorded in 2015, and a second Pb-Pb run will take place at the end of 2018. During the heavy-ion period in autumn 2016, proton-lead collisions were recorded which do not only provide a reference for the Pb-Pb system but are also interesting in their own right. Collisions were recorded at two collision energies: a first period was devoted to 5.02 TeV per nucleon pair to match the energy of the Pb-Pb run and to increase the statistics of the p-Pb data sample recorded in 2013 with a new minimum bias data sample. Collisions at the highest reachable energy of 8 TeV were recorded in a second period at high interaction rate, with triggers from the muon system, the calorimeters and the transition radiation detector.

The LHC produced for the first time collisions of xenon nuclei at a center-of-mass energy of 5.44 TeV during a pilot run with 6 hours of stable beams in October 2017. The remaining time was dedicated to proton-proton collisions at 13 TeV in order to collect a high-statistics data sample with a reach up to highest transverse momenta. A high-multiplicity trigger enables the study of features of events that resemble aspects typical of heavy-ion collisions.

interpolated pp reference spectrum (top panel) and systematic uncertainties (bottom panel).

Until April 2018, ALICE has published 198 peer reviewed scientific papers, with an average of 93 citations each.

The GSI ALICE group is deeply involved in Run-2, starting from the responsibility to continuously operate the Time-Projection-Chamber (TPC) and the participation in the mandatory shifts to operate the experiment at CERN, up to the calibration and analysis of the recorded data and the publication of the results.

The GSI ALICE group is engaged in the analysis of data from all collisions systems and, recently, made public several results of high scientific impact. All relevant results are discussed individually in contributions to this GSI Scientific Report. Here, a brief overview is given.

Transverse momentum spectra and the nuclear modification factor of electrons from semileptonic heavy-flavour hadron decays were measured in Pb-Pb collisions at 5.02 TeV, in Xe-Xe collisions at 5.44 TeV, and in pp collisions at 7 and 13 TeV. At high momenta, the nuclear modification factor is below unity, exhibiting a substantial suppression of the yield of electrons from heavy-flavour hadron decays with respect to pp collisions due to the energy loss of heavy quarks in the QCD medium. Models including shadowing of parton distributions predict a nuclear modification factor below unity even at low momentum and are in better agreement with the data than models without shadowing.

Inclusive and non-prompt production of J/ψ and its centrality dependence was measured in Pb-Pb collisions at 5.02 TeV. Non-prompt J/ψ production originates from the decay of B mesons. Thus both measurements give access to transport coefficients of heavy quarks in the QCD medium. The inclusive measurement confirms the observation in Pb-Pb collisions at 2.76 TeV of a reduced suppression in central collisions when compared to lower energies.

The Xe-Xe data allow for studying the dependence of particle production on the collision system size where xenon neatly bridges the gap between existing data from pp, p-Pb and Pb-Pb collisions with atomic mass numbers of $A=129$ for xenon, and $A=208$ for lead. Figure 1 shows the transverse momentum spectra of charged particles in Xe-Xe collisions at 5.44 TeV in nine centrality classes together with an interpolated pp reference spectrum (top panel) and systematic uncertainties (bottom panel).

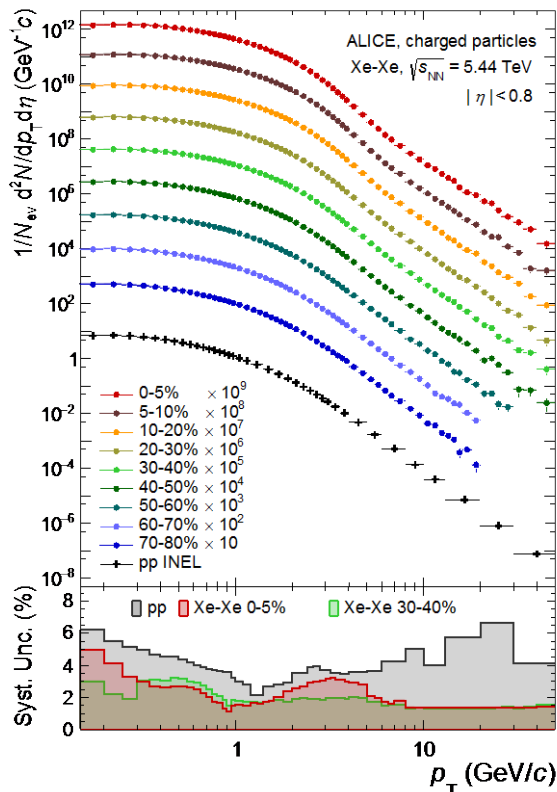


Figure 1: Transverse momentum spectra of charged particles in Xe-Xe collisions at 5.44 TeV together with an

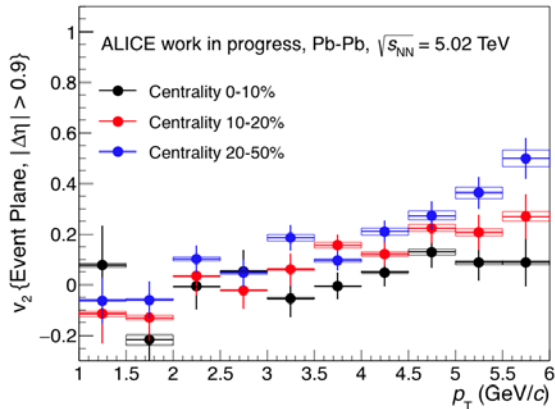


Figure 2: Elliptic flow coefficient (v_2) of ^3He in Pb-Pb collisions at 5.02 TeV.

The elliptic flow coefficient (v_2) of (anti)- ^3He was measured versus transverse momentum in Pb-Pb collisions at 5.02 TeV for different centrality ranges using the Event Plane method, see Fig. 2. This measurement decisively adds to the picture obtained from the v_2 of (anti)-deuterons and (anti)-protons and poses a serious challenge to the coalescence approach and other hadronization models that describe the elliptic flow of light anti-nuclei in heavy-ion collisions.

The GSI ALICE group is centrally involved in the preparation of the experiment upgrades, to be completed until the end of 2020. These upgrades will allow ALICE to fully exploit the improved performance of the LHC in Run-3, when Pb nuclei will collide with a rate of 50 kHz.

The construction of new readout chambers for the ALICE TPC, equipped with Gas Electron Multiplier (GEM) foils is at full swing.

A pre-production GEM-based Inner Readout Chamber (IROC) has been tested together with 6 prototype versions of the TPC front-end card based on SAMPA version ‘v2’ at the CERN Proton Synchrotron with electrons and pions at 1 to 6 GeV/c.

The measured noise and separation power in particle identification meet the design specifications. Groups of two detectors, i.e. one Inner and one Outer Readout Chamber (OROC), are placed close to the LHC beam pipe at about 10 m from the interaction point in the ALICE cavern, where particle densities are about one order of magnitude higher than those expected in the TPC chambers in Run-3 at a 50 kHz Pb-Pb collision rate. Figure 3 shows one OROC being positioned below the beam pipe at the ALICE experiment.

Final production chambers were thus exposed to the LHC conditions at forward rapidity under nominal gas and high voltage conditions without any trips during several weeks of operation. However, minor discharges were observed.

Plans for 2018 are to periodically install in the ALICE cavern sets of four readout chambers – two inner readout chambers and two outer ones-, operate them for several weeks, and then replace them during technical stops or other suitable opportunities, in order to qualify a meaningful sub-set of the full production for the final installation for Run-3 operations at the LHC.

*Work supported by BMBF, GSI.

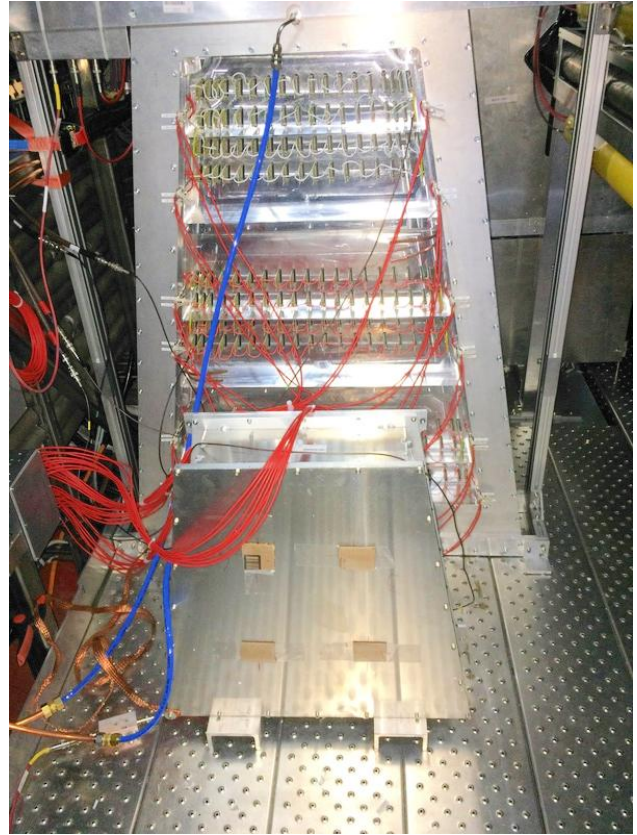


Figure 3: Four chambers (two inner and two outer readout chambers) placed close to the LHC beam pipe in the ALICE cavern ready to be operated with beams.

CATS - the modern tool for femtoscopy studies

V. Mantovani Sarti¹, D.L. Mihaylov¹ and L.Fabbietti^{1,2}

¹Physics Department E62, TUM, Garching, Germany; ²Excellence Cluster Universe, Garching, Germany

Femtoscopy relates the correlation function $C(k)$ between particle pairs to their emission source $S(r, k)$ and the wave function $\Psi(r, k)$. The latter is obtained by solving the Schrödinger equation (SE) for an interaction potential $V(r)$.

Investigating small collision systems, such as proton-proton, has the advantage of probing the inner part of the interaction potential. However, modelling the correlation function for small sources requires an exact determination of the wave function, which is not provided by the common femtoscopy tools developed for investigating correlations in heavy-ion collisions. For this reason, we have developed a new ‘‘Correlation Analysis Tool using the Schrödinger equation’’ (CATS) [1] capable of modelling $C(k)$ exactly using a numerical solution to the SE.

CATS was used to fit the ALICE experimental results for p-p and p- Λ correlations in pp collisions at $\sqrt{s} = 7\text{TeV}$. The source was assumed to be Gaussian and the size was extracted from a combined fit of the p-p and the p- Λ correlations. Both systems show the presence of a linear baseline, which is not reproduced by transport models. Thus, the fit is performed by multiplying $C(k)$ with a linear function. The result is shown in fig. 1.

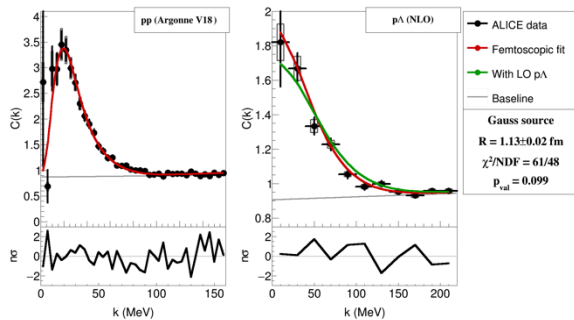


Figure 1: The ALICE preliminary, pp at $\sqrt{s} = 7\text{TeV}$ [2] was fitted using CATS to model the p-p correlation function. The p- Λ interaction was evaluated with the Lednicky model [3] using the scattering parameters of a next to leading order (NLO) chiral effective theory calculation [4].

For more exotic pairs, such as hyperon-hyperon or hyperon-nucleon in the $S = -2$ sector, the correlation function $C(k)$ permits to gain access to the underlying strong interaction, which so far has not been fully constrained by scattering or hypernuclei data. We expect to be able to use the ALICE pp data at $\sqrt{s} = 13\text{TeV}$ to get an insight into the Λ - Λ and p- Ξ^- correlations (fig. 2). For this purpose, we established collaborations with theory groups working on chiral effective field theory and lattice calculations, allowing us to probe the most modern potentials for different particle species and make predictions about the feasibility to study those pairs experimentally.

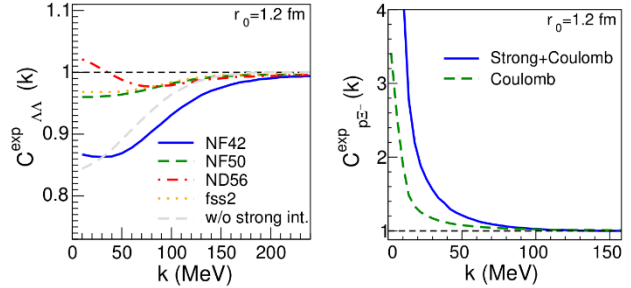


Figure 2: The predicted experimental correlation function for Λ - Λ (left) and p- Ξ^- (right), including momentum resolution and feed-down effects expected in pp collisions at LHC energies.

In the left panel of Fig. 2 we compare the Λ - Λ correlation functions for different attractive (NF50, ND56 and fss2) potentials and one potential (NF42) which allows for a bound state [5]. The binding potential (NF42) is well separated from the attractive ones, which implies that a high statistics experimental data sample can differentiate between those cases. For the p- Ξ^- (right) we use a preliminary lattice local potential from the HAL QCD collaboration [6]. We see a significant modification of $C(k)$ due to the strong interaction, which should be possible to detect experimentally.

To get better constraints on the investigated interaction potentials, we are working on a CATS based analysis framework capable of performing global fits over all available femtoscopy data.

The work on CATS and the complementary studies are in preparation for publication and currently to be found on arXiv [1].

This work is supported by SFB1258.

References

- [1] D. L. Mihaylov, V. M. Sarti, O. W. Arnold, L. Fabbietti, B. Hohlweiger and A. M. Mathis, arXiv:1802.08481 [hep-ph].
- [2] O. Arnold [for the ALICE collaboration], poster at the QM2017 conference.
- [3] R. Lednicky and V. L. Lyuboshits, Sov. J. Nucl. Phys. 35 (1982) 770 [Yad. Fiz. 35 (1981) 1316].
- [4] J. Haidenbauer, S. Petschauer, N. Kaiser, U.-G. Meissner, A. Nogga and W. Weise, Nucl. Phys. A 915 (2013) 24 doi:10.1016/j.nuclphysa.2013.06.008 [arXiv:1304.5339 [nucl-th]].
- [5] A. Ohnishi, K. Morita, T. Furumoto, JPS Conf. Proc. 17 (2017) 031003 doi:10.7566/JPSCP.17.031003 [arXiv:1512.08444 [nucl-th]].
- [6] T. Hatsuda, K. Morita, A. Ohnishi and K. Sasaki, Nucl. Phys. A 967 (2017) 856 doi:10.1016/j.nuclphysa.2017.04.041 [arXiv:1704.05225 [nucl-th]].